Recent Developments in RheoSANS

Katie Weigandt (NIST)

June 7th 2017

canSAS Workshop

Acknowledgements

Steve Hudson (NIST)
Javen Weston (NIST, Georgetown U)
Daniel Seeman (NIST)
Paul Salipante (NIST)
Daniel Blair (Georgetown U)

Lionel Porcar (ILL)
Joao Cabral (Imperial College London)

Matt Helgeson (UC Santa Barbara)
Nino Ruocco (UC Santa Barbara)
Patrick Corona (UC Santa Barbara)

Carlos Lopez-Barron (Exxon-Mobile)
Jeff Richards (NIST)

Lynn Walker (Carnegie Mellon)
Blake Bleier (Carnegie Mellon)

Funding: nSoft, NIST IMS

RheoSANS -- Introduction

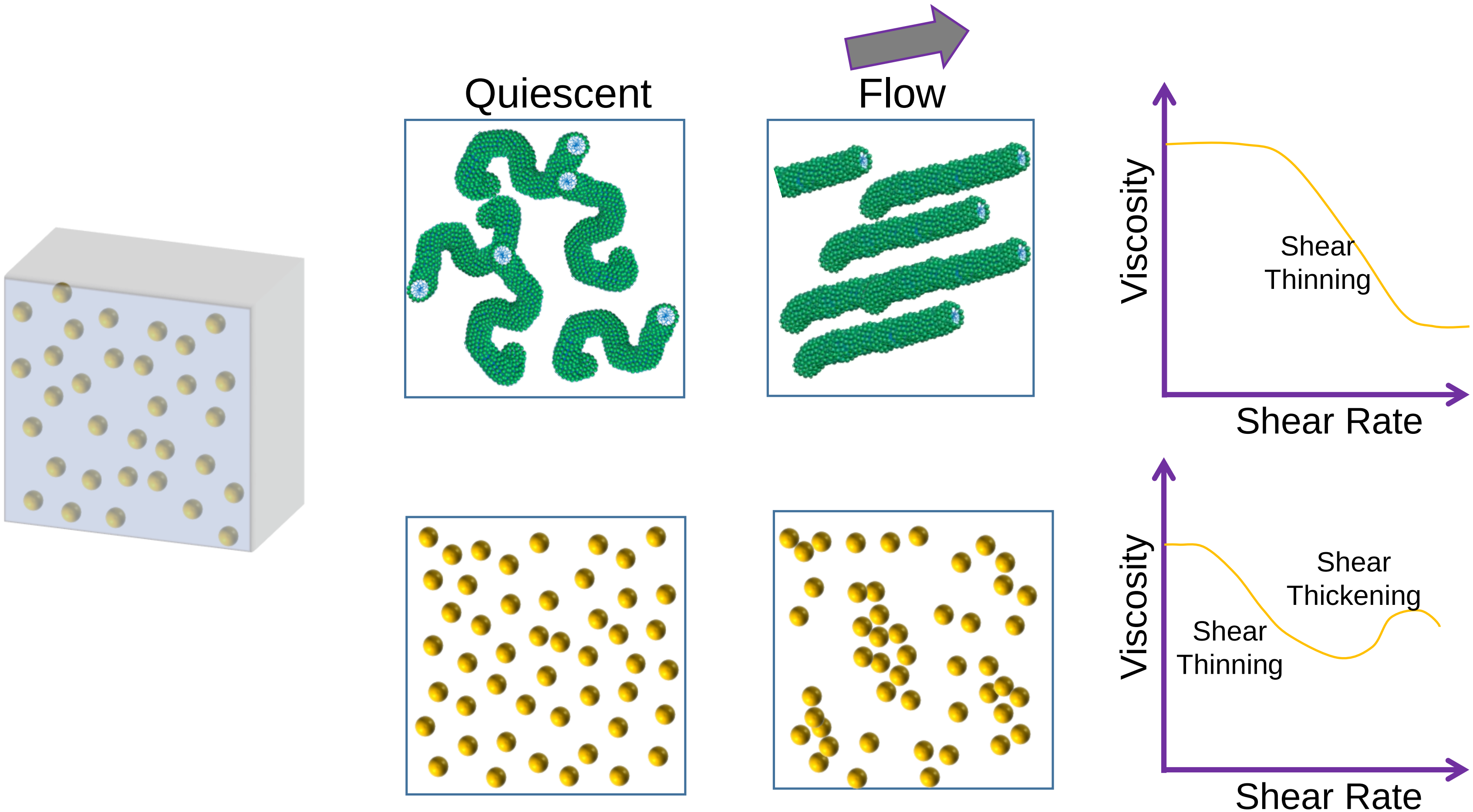

Current Opinion in Colloid & Interface Science 17 (2012) 33–43

Flow-SANS and Rheo-SANS applied to soft matter

Aaron P.R. Eberle [a], Lionel Porcar [b,*]

[a] NIST Center for Neutron Research, National Institute of Standards and Technology, Gaithersburg, MD, 20899, USA
[b] Large Scale Structure Group, Institut Laue Langevin, Grenoble, France

RheoSANS-Status quo

RheoSANS

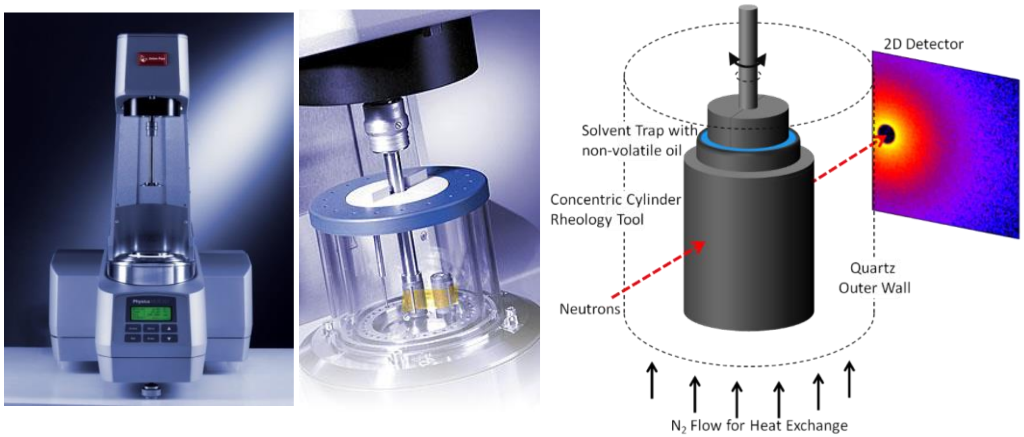

L. Porcar (NIST), J. Moyer (NIST), P. D. Butler (NIST), L. D. Pozzo (NIST, UW)
G. Langenbucher (Anton Paar)

1–2 Plane Shear Cell

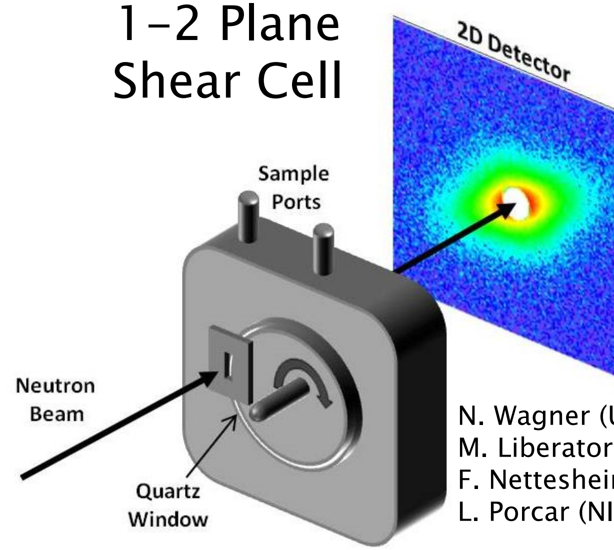

N. Wagner (UDel)
M. Liberatore (UDel)
F. Nettesheim (UDel)
L. Porcar (NIST)

Extensional Flow Cell

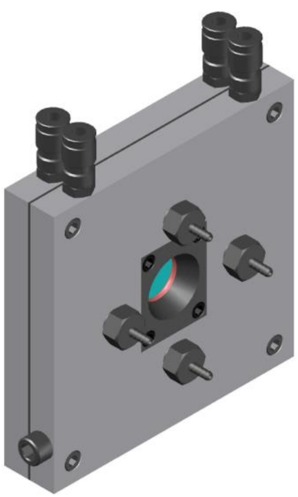

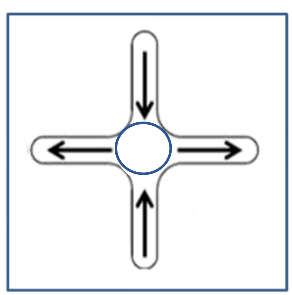

K. Weigandt (NIST)
Koty McAllister (UDEL)

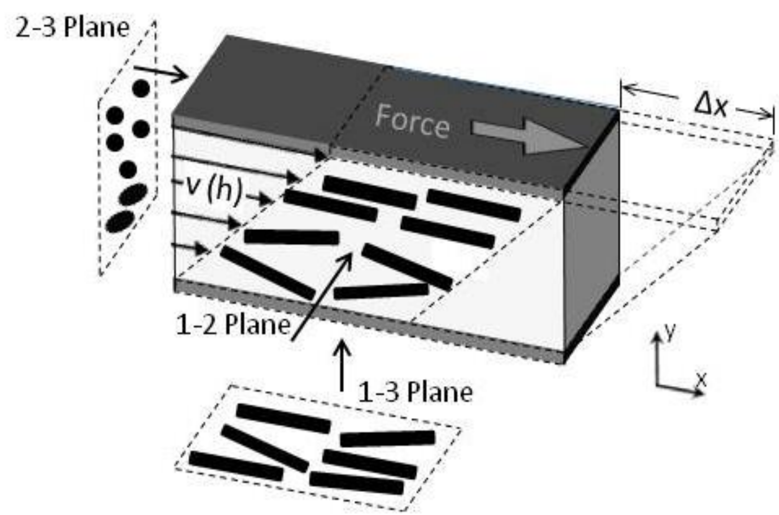

Measure Simultaneous Rheology, Structure and…

Dielectric RheoSANS: Motivation

Carbon Black Suspensions for Flow Battery Electrodes

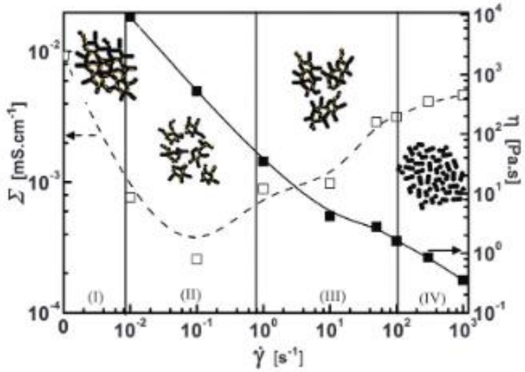

Youssrey et al. Chem. Phys (2013) 15, 14476

Ion Conduction through Self-Assembled Porous Materials Ordered by Flow

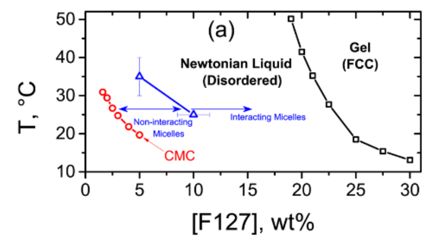

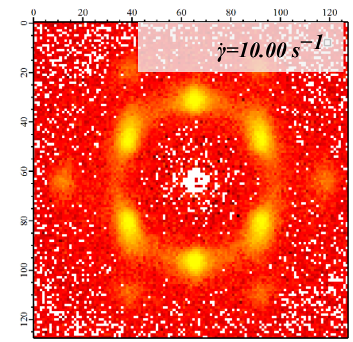

Lopez-Barron et al. Macromolecules (2014) 47.7484

Next Generation Conductive Additives

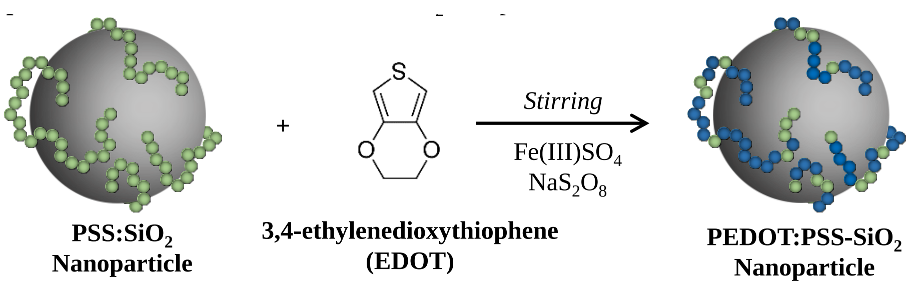

Richards et al. ACS Applied Materials and Interfaces (2016)

Self-Assembled Semiconducting Nanofibers

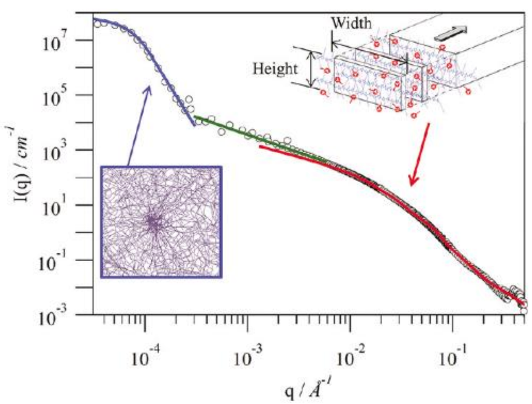

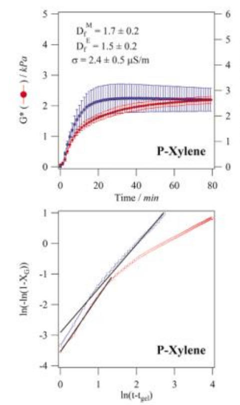

Newbloom et al. Macromolecules (2012) 45.3452-3462

Jeff Richards et al

Dielectric RheoSANS: Experiment

Dielectric RheoSANS Geometry

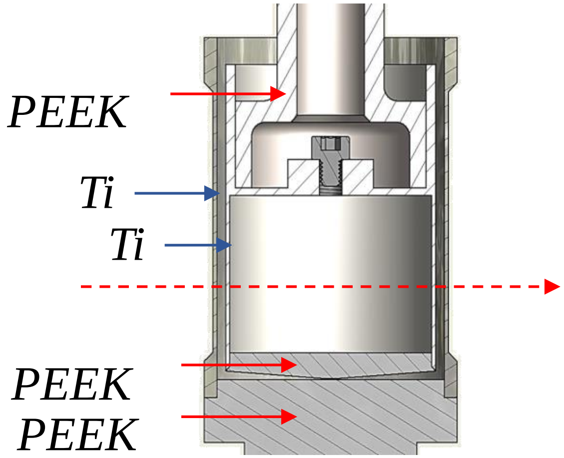

ARES G2 Synchronization Protocol

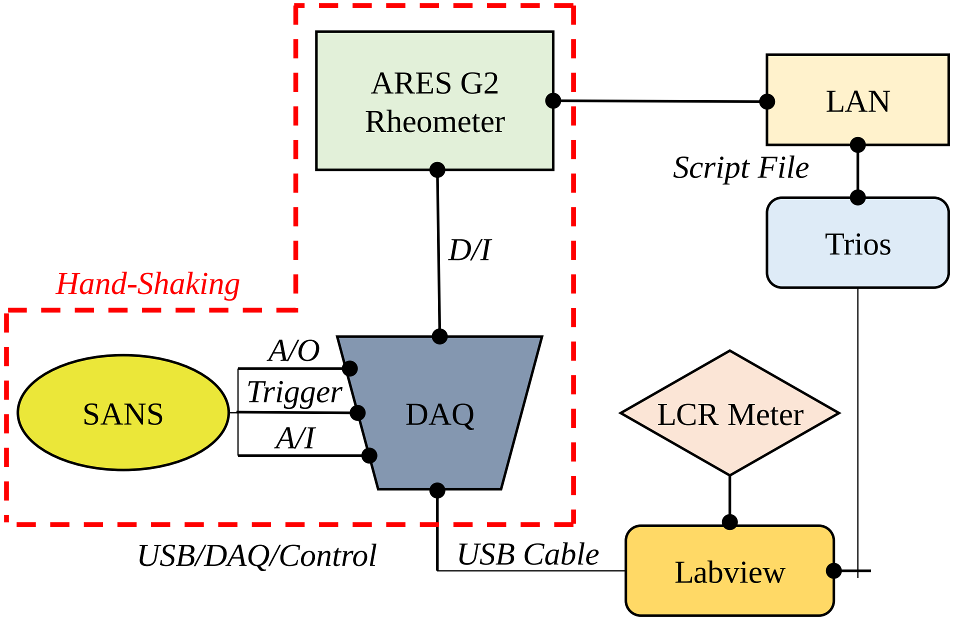

Modified Oven Cross-Section

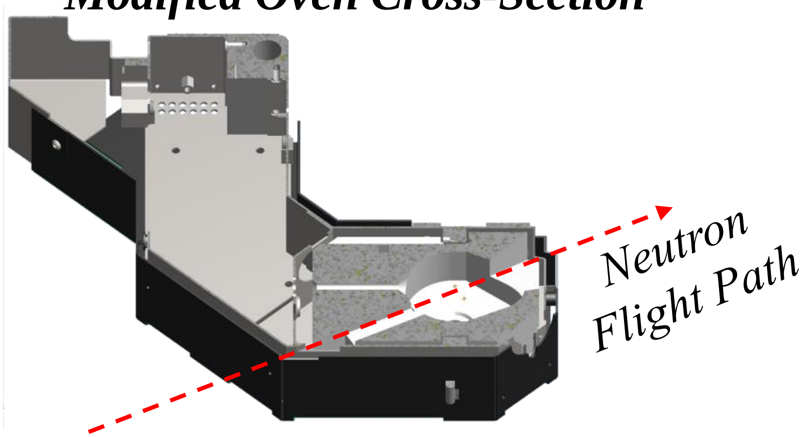

Strain-Controlled Sample Environment

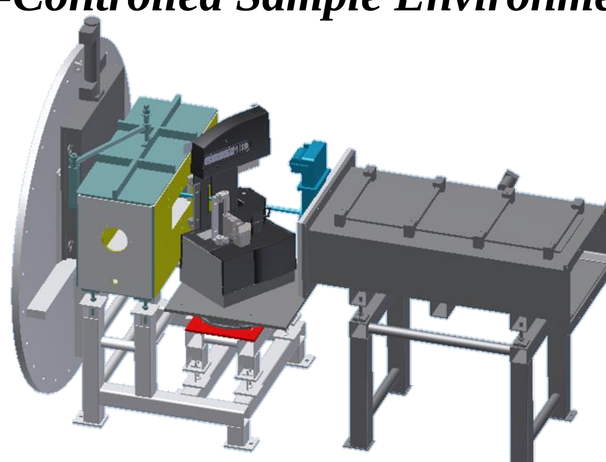

*Richards J. J. et al, "*Dielectric RheoSANS – Simultaneous Interrogation of Impedance, Rheology and Small Angle Neutron Scattering of Complex Fluids*" 2017 JoVE in press.*

Other Rheometer Options (Extensional Strain)

Extensional Strain

Example 1: Thermoplastic Elastomers (TPEs)

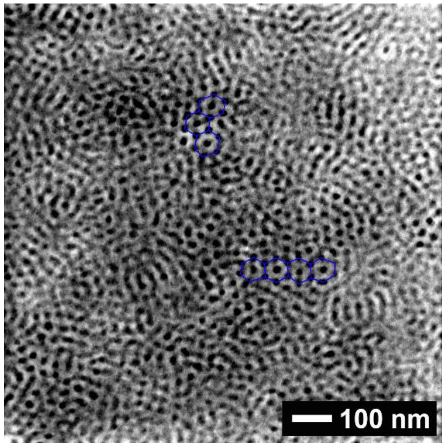

TPE:
SIS triblock copolymer

Stretched at
room temperature

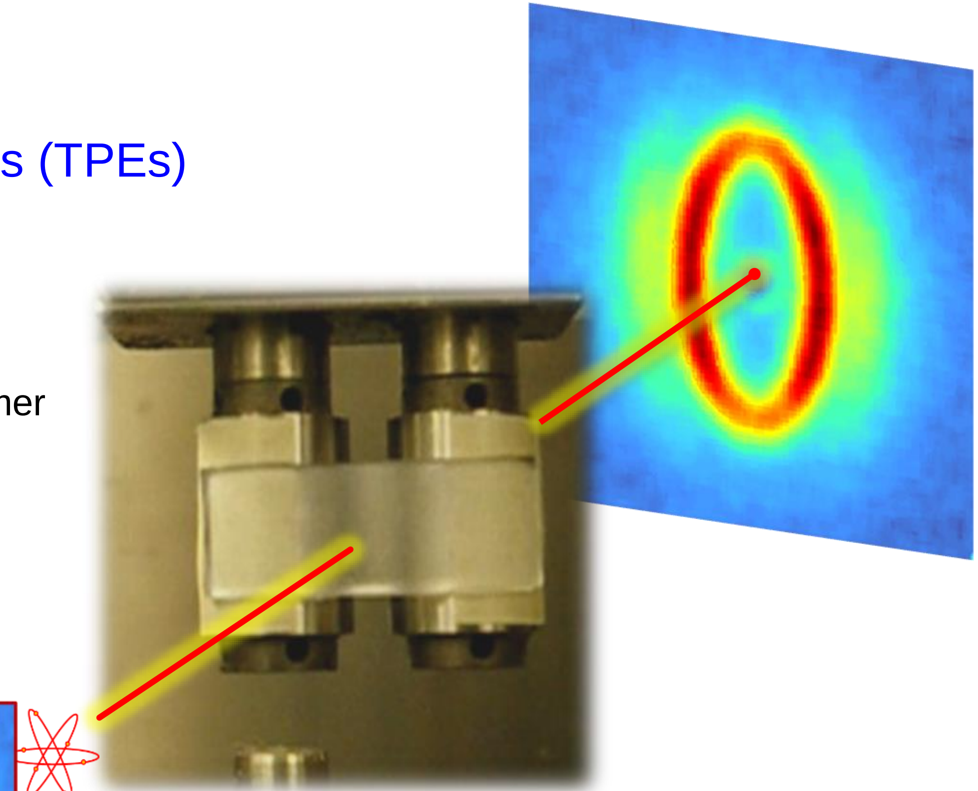

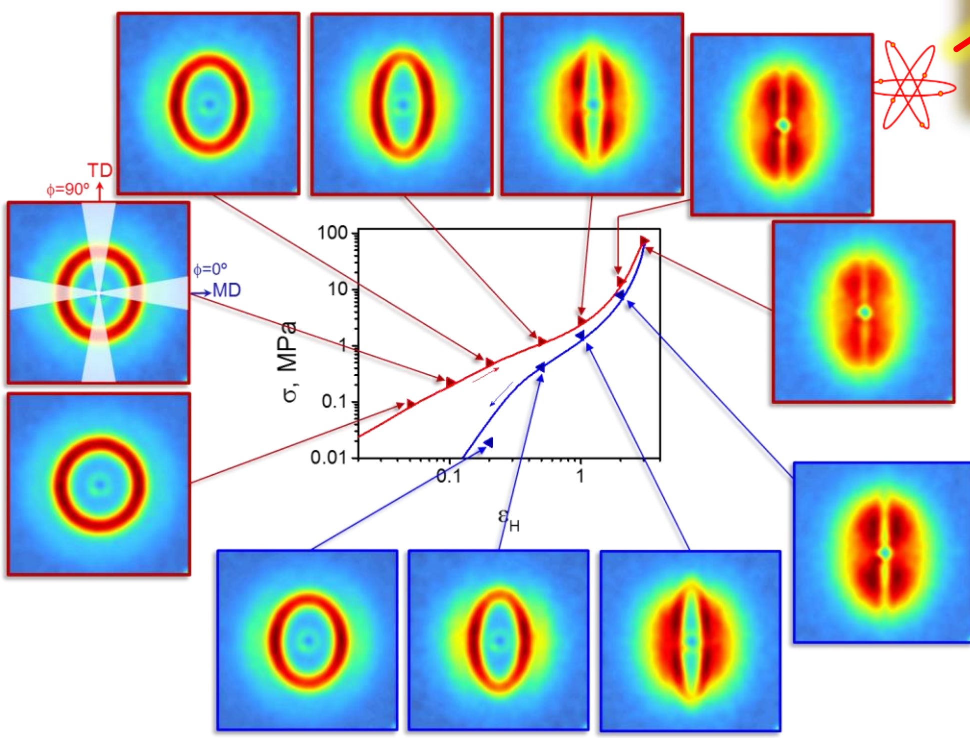

Sentmanat Extensional rheometer (SER):

Ideal geometry for *in-situ* scattering measurements

López-Barrón et al., *Rheol. Acta* **55**, 103 (2016)

Extensional Strain

Example 3: Polymer melts

Sample: Polystyrene (H/D Isotope blends

Stretched in the melt (at 150 °C) using time-resolved SANS

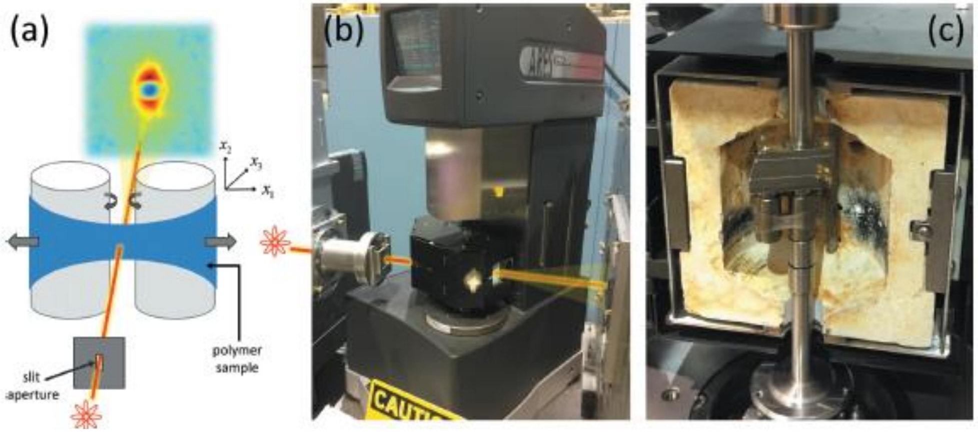

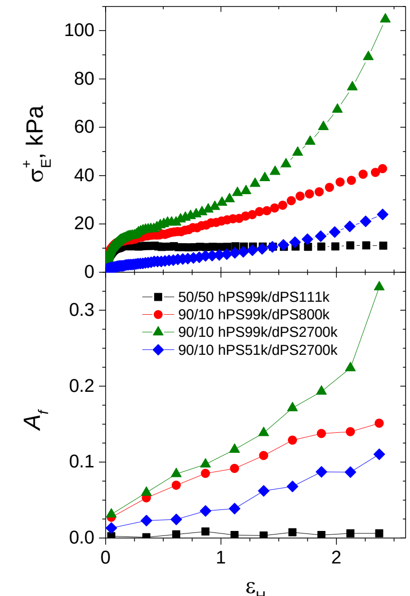

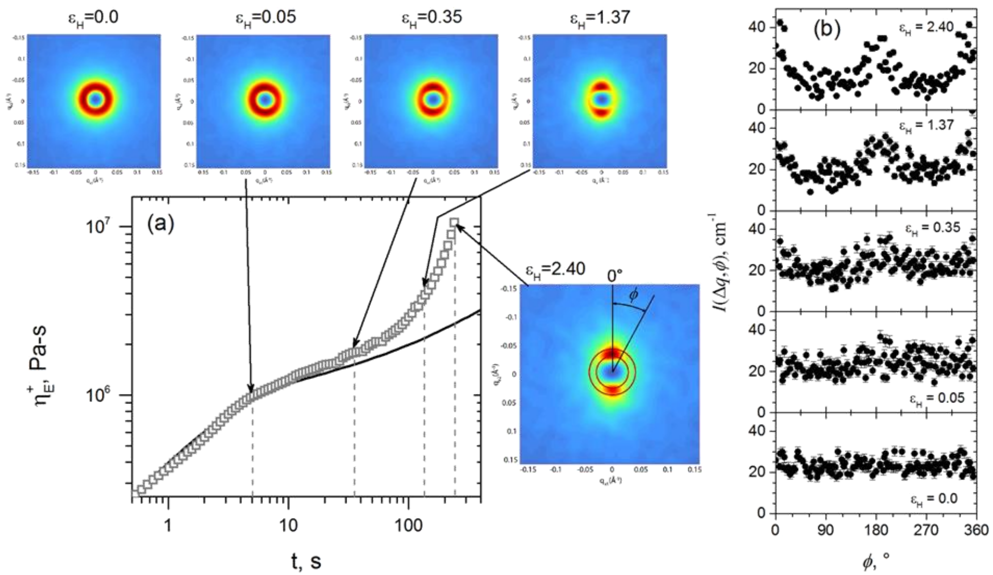

Stress-SANS rule (analogous to stress-optic rule):

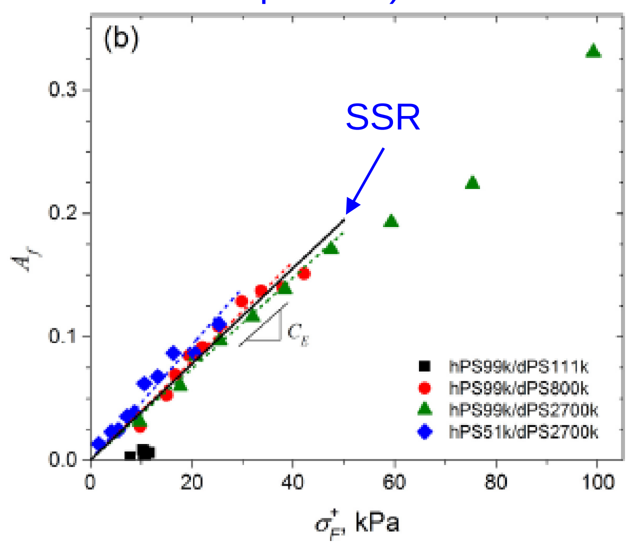

López-Barrón et al., *J. Rheol.* **61**, 697-710 (2017)

Realistic and Industrially Relevant Flow Conditions

It is often very difficult to measure the nanostructure of complex fluids in dynamic and industrially relevant environments!

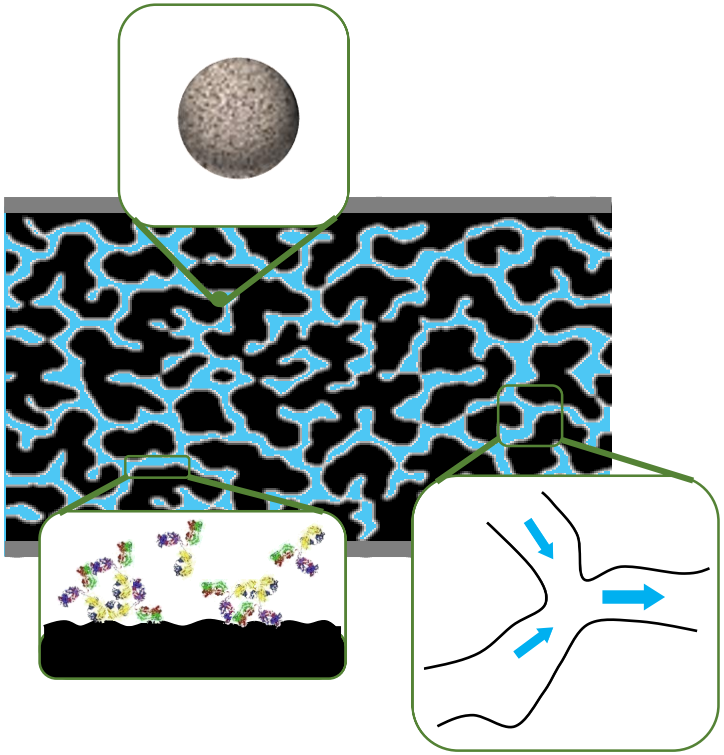

High Strain/Flow Rates
(~1,000,000 s^{-1})

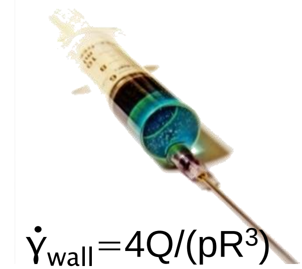

Non-Ambient Conditions

High Temperatures
(>200°C)

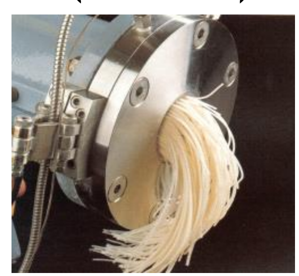

and

High Pressures
(up to 70 MPa)

Toward *real* processing flows

Real processing flows involve a range of deformation types and histories.

Injection molding

*R. Svečko et al., **Sensors**, 2013, 13(5).*

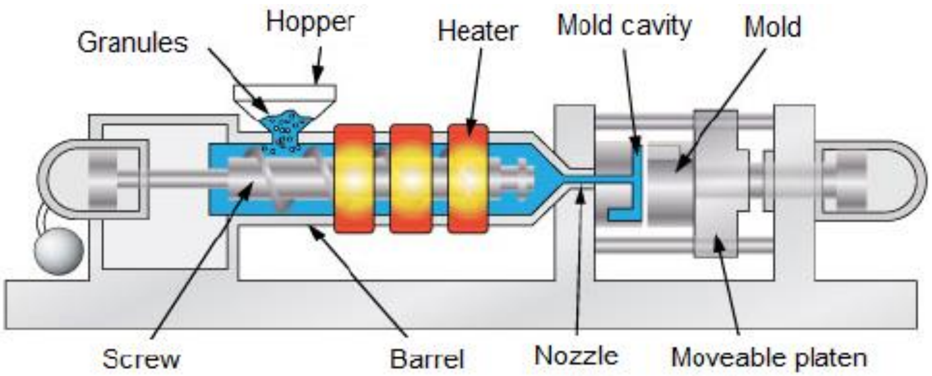

Hydraulic fracturing

Indiana Geological Survey

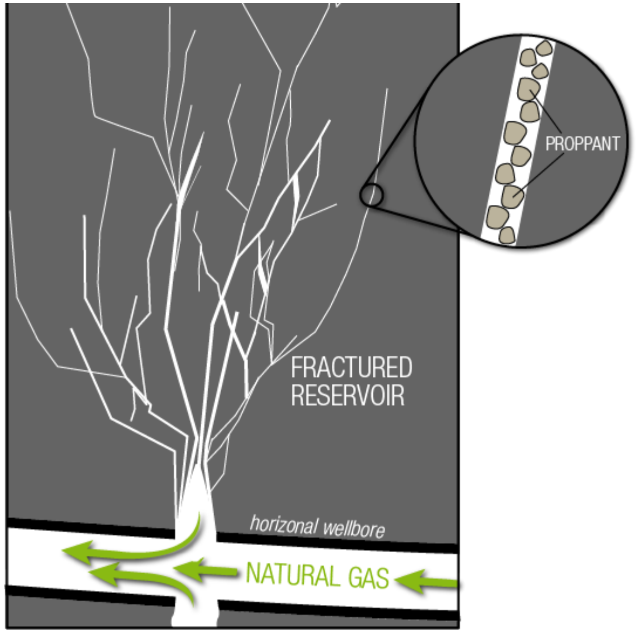

3D printing

B.Y. Ahn et al., Science, 2009, 323(5921).

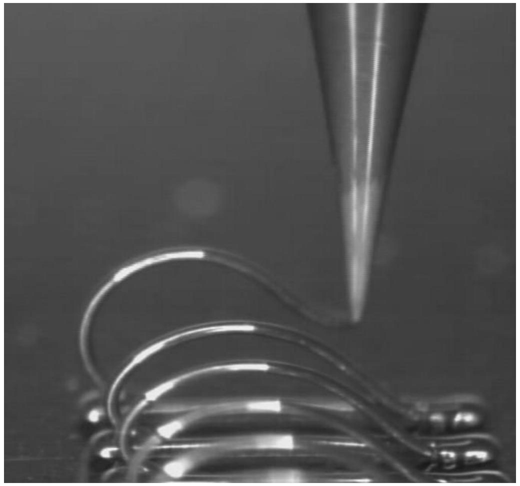

A fluidic four-roll mill (FFoRM) for arbitrary deformations

Fluidic four-roll mill (FFoRM)

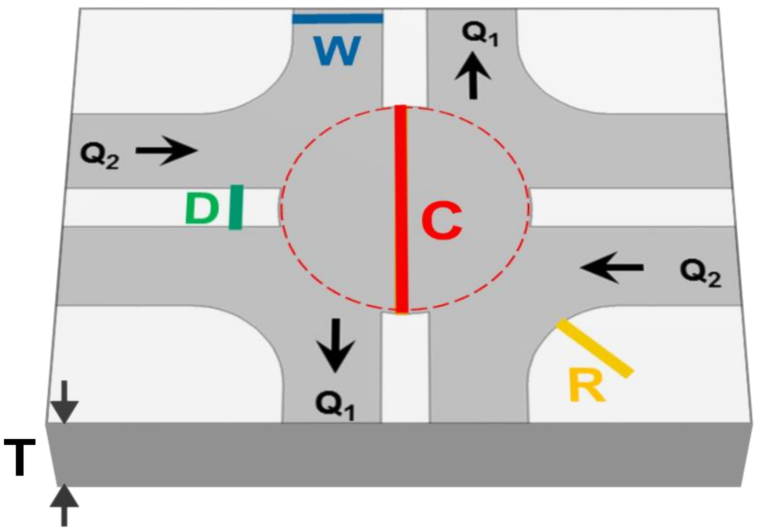

Advantages over other designs:

- Uniform, Lagrangian-steady deformation type/rate
- Long residence time in beam area (steady state)
- Λ and $\dot{\Gamma}$ can be arbitrarily varied in time

Straining in an arbitrary 2D flow

$$\dot{\Gamma} = \frac{1}{2}(\nabla \underline{u} + \nabla \underline{u}^{T})^{1/2} = \frac{\dot{\Gamma}}{2}\begin{bmatrix} \Lambda & 1-\Lambda \\ 1-\Lambda & \Lambda \end{bmatrix}$$

Flow type parameter: $\Lambda = \Lambda(Q_2/Q_1)$
Rate of strain: $\dot{\Gamma} = \dot{\Gamma}(Q_1)$

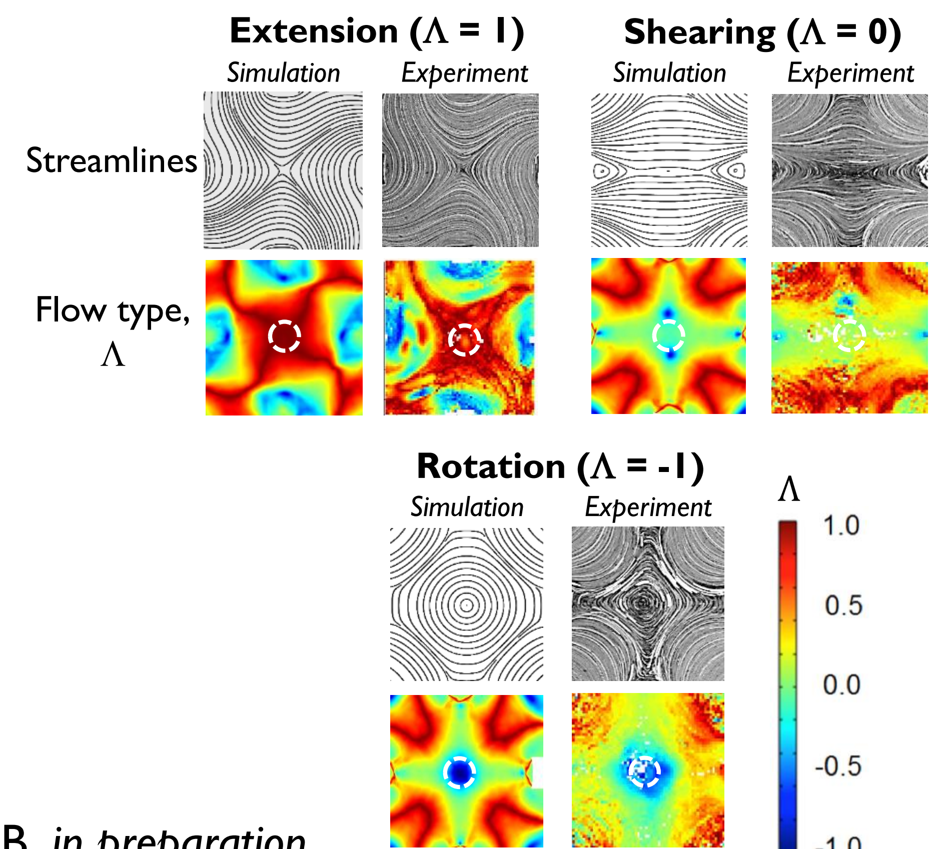

(white circles are 1 mm)

Helgeson group, UCSB, *in preparation.*

Model test fluid – colloidal rod suspensions

Cellulose nanocrystals
(3.3 vol% in D_2O)

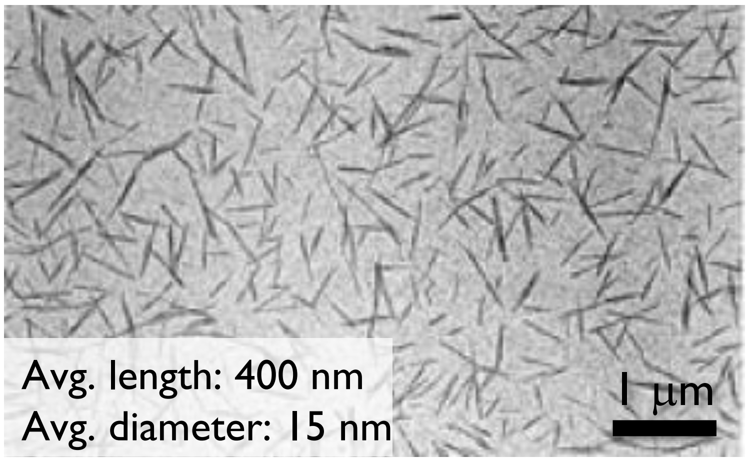

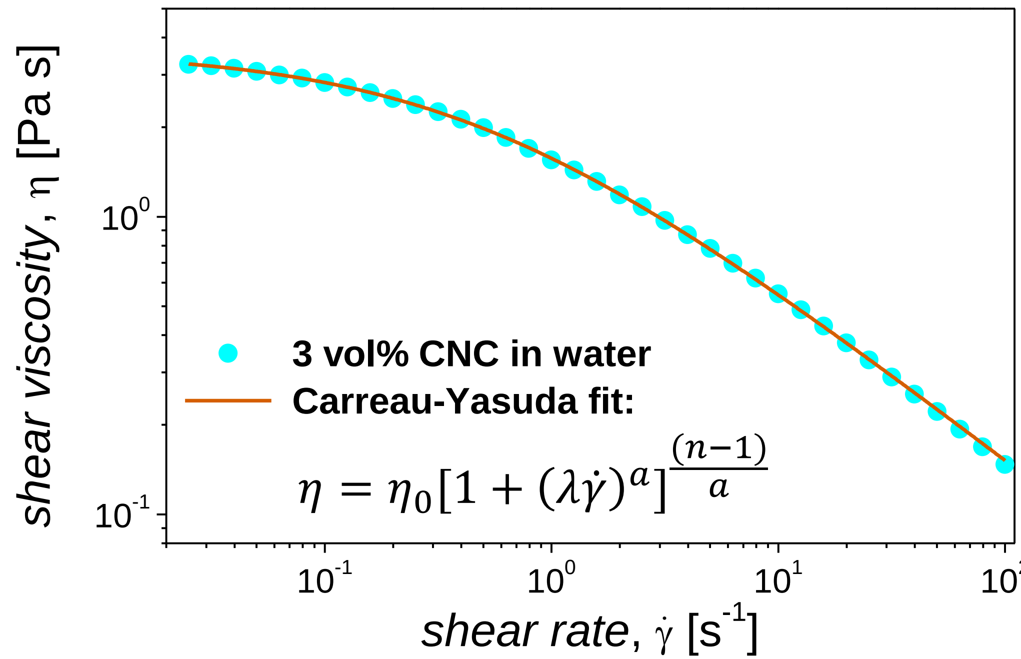

Exact microscopic theory for dilute colloidal rod suspensions[1]

Dilute rods in 2D flow: $$\theta_0(\Lambda) = \text{acos}\left(\sqrt{\frac{1}{2} + \frac{\sqrt{\Lambda}}{1+\Lambda}}\right)$$

[1] Bird, Armstrong, Hassager and Curtiss, Dynamics of Polymeric Liquids, Wiley, 1977.

UC SANTA BARBARA chemical engineering

Helgeson group, UCSB, *in preparation.*

It is often very difficult to measure the nanostructure of complex fluids in dynamic and industrially relevant environments!

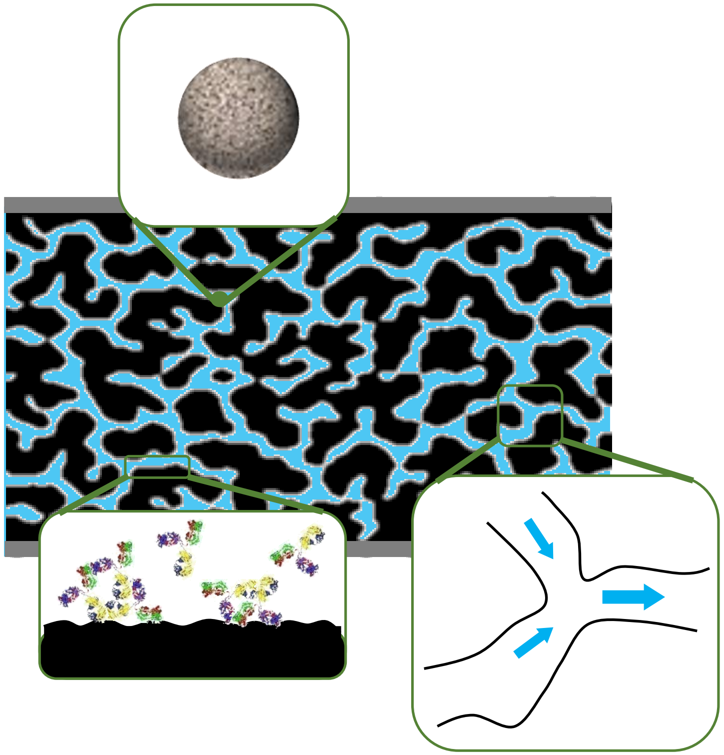

High Strain/Flow Rates
(~1,000,000 s^{-1})

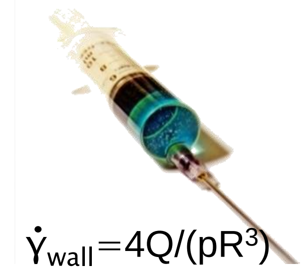

Non-Ambient Conditions

High Temperatures
(>200°C)

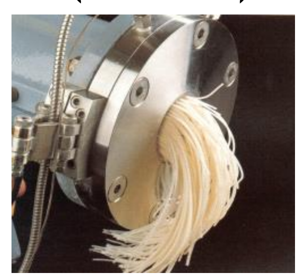

and

High Pressures
(up to 70 MPa)

µRheoSANS -- Requirements

RheoSANS

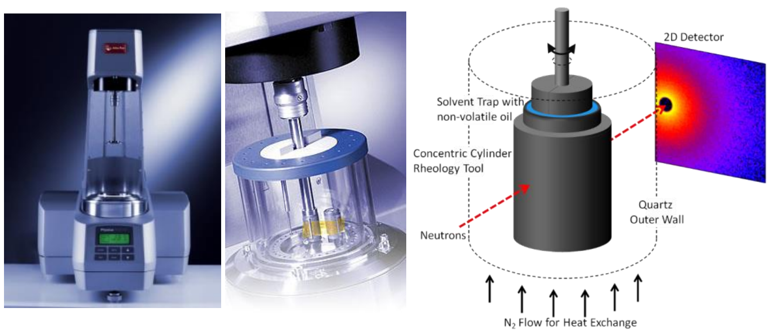

L. Porcar (NIST), J. Moyer (NIST), P. D. Butler (NIST), L. D. Pozzo (NIST, UW)
G. Langenbucher (Anton Paar)

Desired Capabilities

Temperature	**>200°C**
Pressure	**up to 70 MPa**
Shear Rate	**up to 10^6 s^{-1}**

RheoSANS Capabilities

Temperature	**-50°C to 200°C**
Pressure	**Atmospheric**

High Shear Rate + Low Shear Stress

- Shear Rate **12,000 s^{-1}**
- Shear Stress **900 Pa**

Low Shear Rate + High Shear Stress

- Shear Rate **3,500 s^{-1}**
- Shear Stress **4,500 Pa**

Pressure Driven Flow/Capillary Rheometry

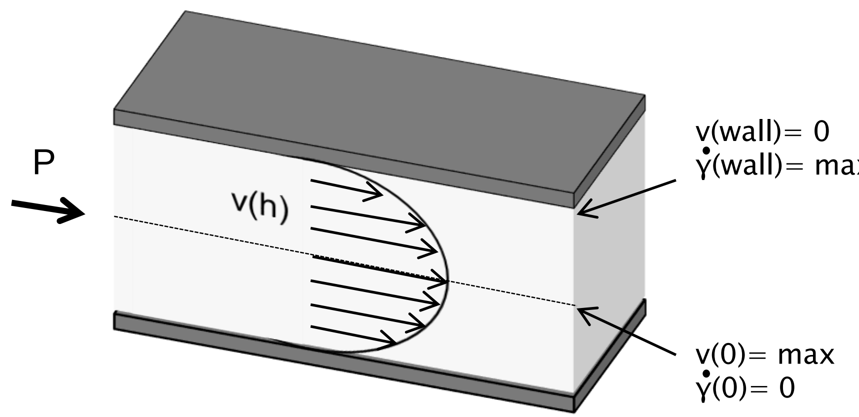

µRheoSANS -- Prototype

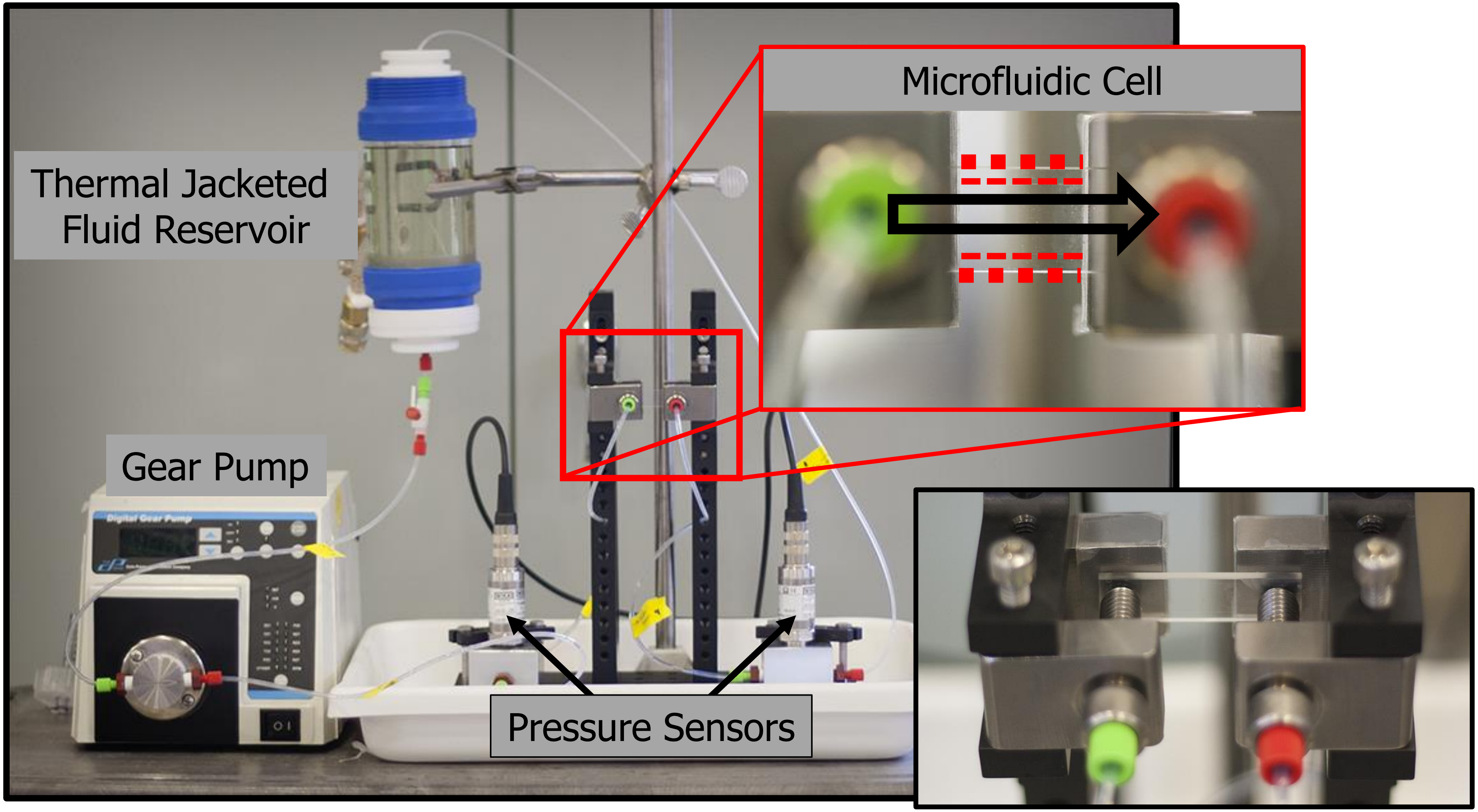

Weston, Seeman, Salipante, Blair, Hudson and Weigandt (In Preparation)

µRheoSANS of Anionic Wormlike Micelles

1.15% Steol CS460/8% NaCl in D_2O

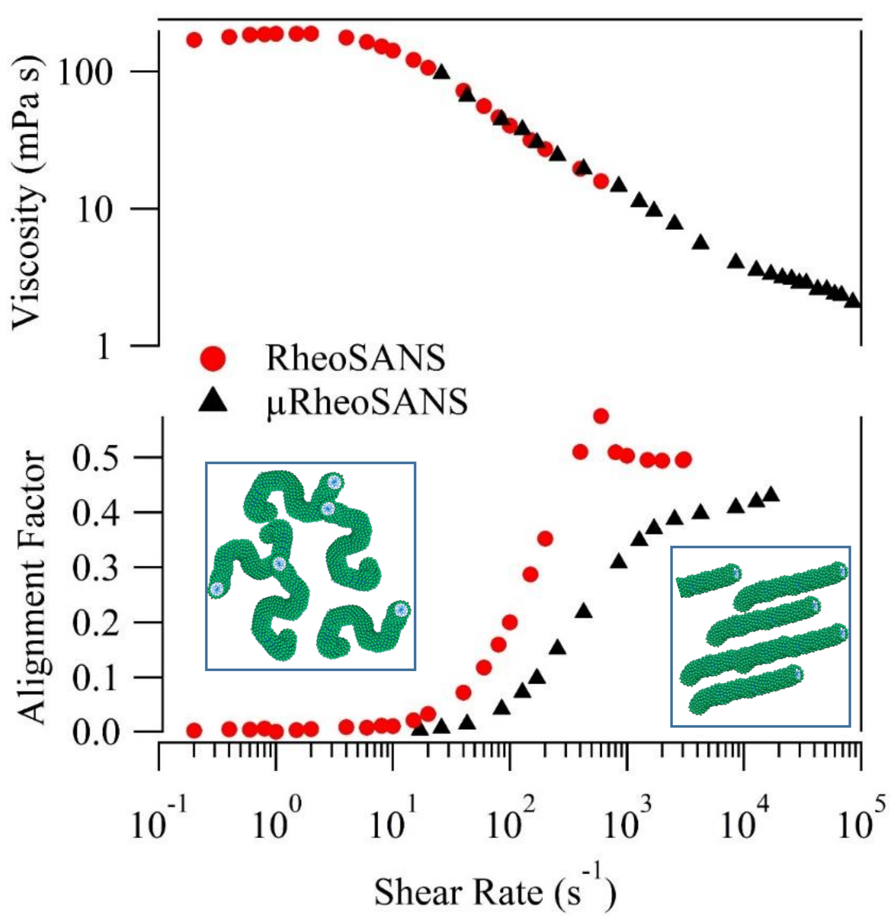

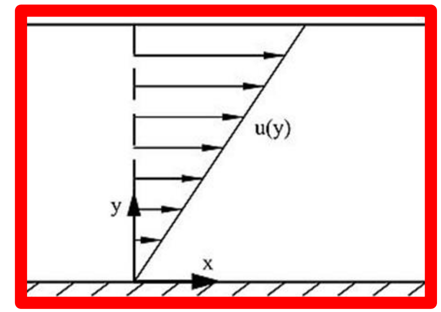

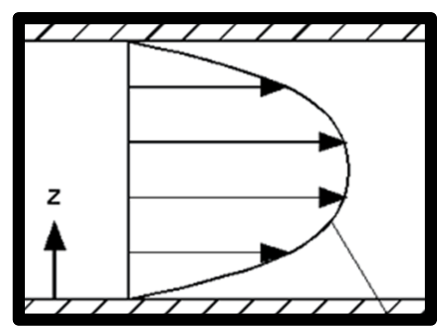

Couette vs Poiseuille RheoSANS

$$\frac{d}{dy}(\text{velocity}) = \dot{\gamma} = \text{constant}$$

COUETTE FLOW

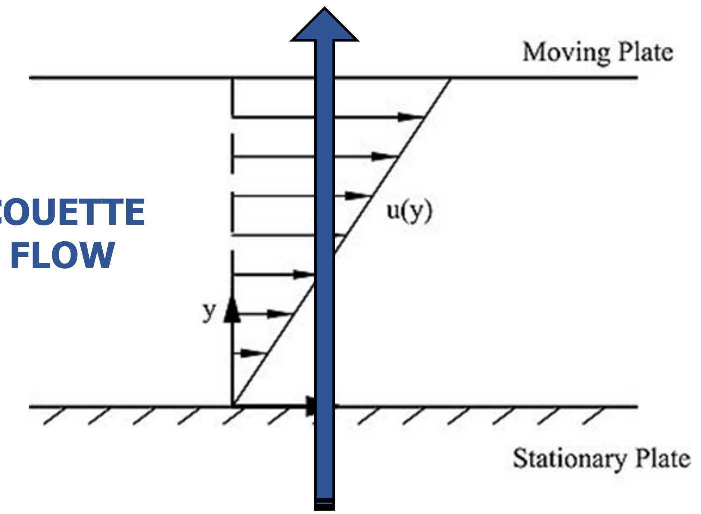

NEUTRON BEAM

$$\frac{d}{dy}(\text{velocity}) = \dot{\gamma} = f\,(y, \Delta P, h, w, \eta, \ldots)$$

POISEUILLE FLOW

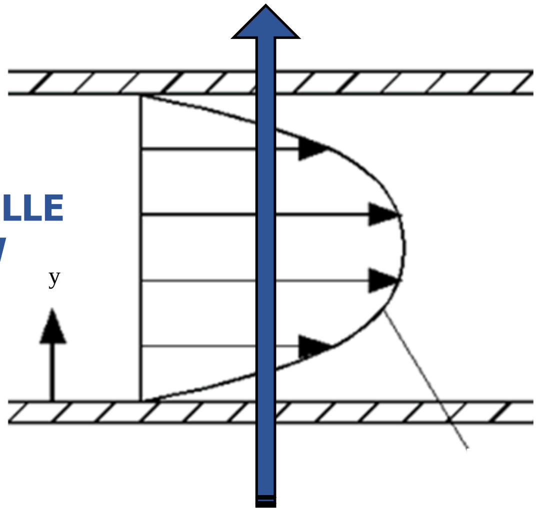

NEUTRON BEAM

How can we deconvolute the scattering patterns resulting from Poiseuille Flow RheoSANS?

High shear SANS in rectangular channels

- How to isolate a certain stress, when a whole spectrum is present?
  - Depth sectioning method demonstrated by Fernandez-Ballester et al., JoR ’09 (WAXS).
  - Linear stress profile from channel wall to center (continuum)
    - Scattering produced from a superposition of these stress states.
  - When the pressure is increased from one state to another, the difference comes only from the highest stress near the channel walls.

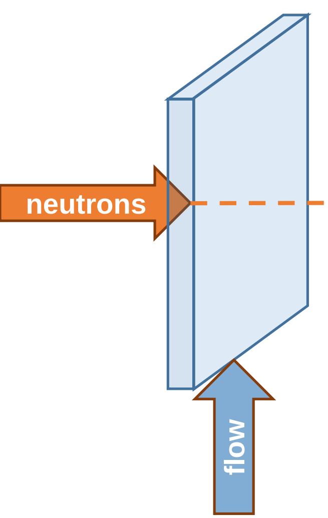

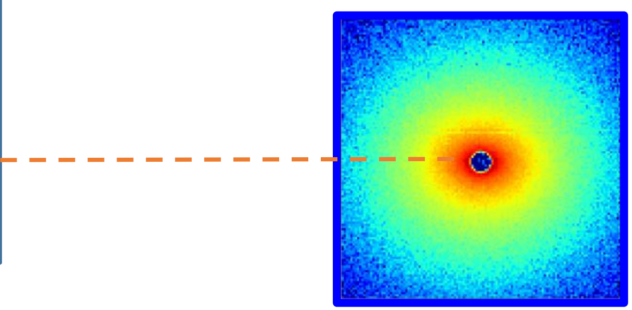

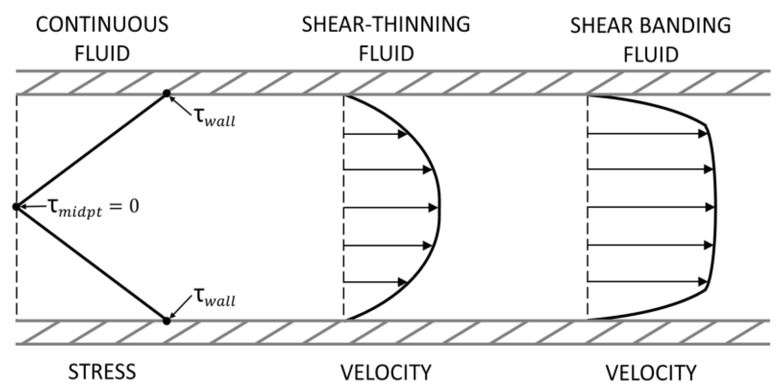

Subtraction based on linear stress profile for continuous fluids

Analysis: Determining Structure near the Wall

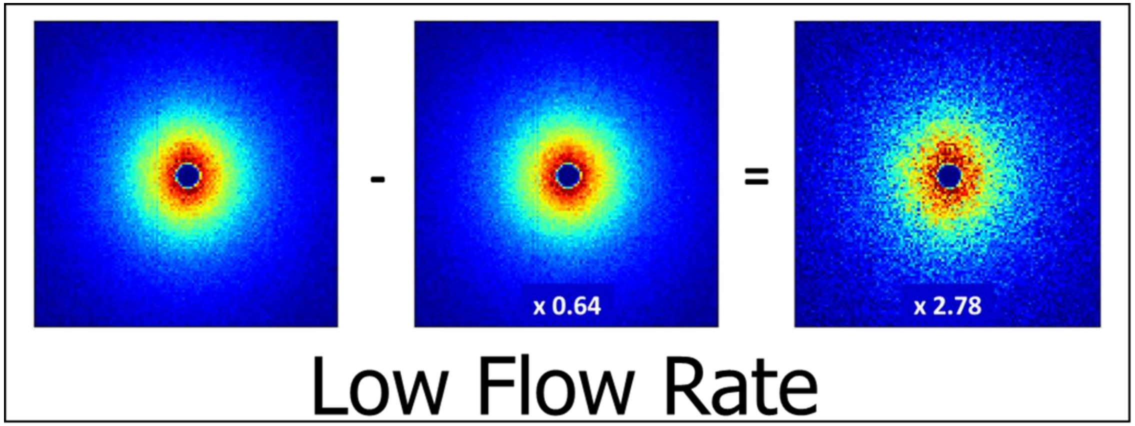

I(q) from entire flow **-** I(q) from a lower wall stress, scaled 64% = I(q) from the top and bottom 18%, and corrected for new scattering volume (x 2.78)

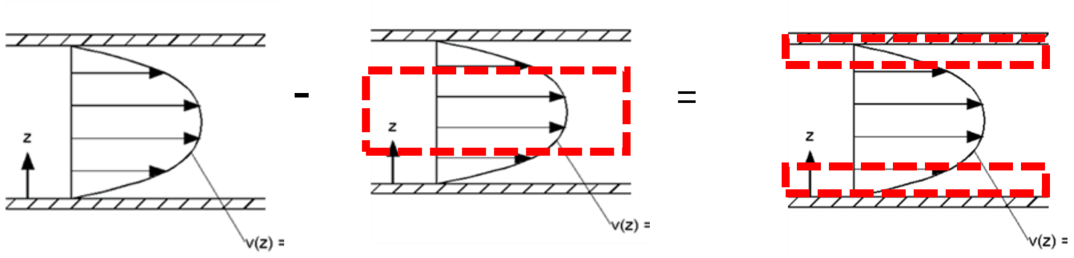

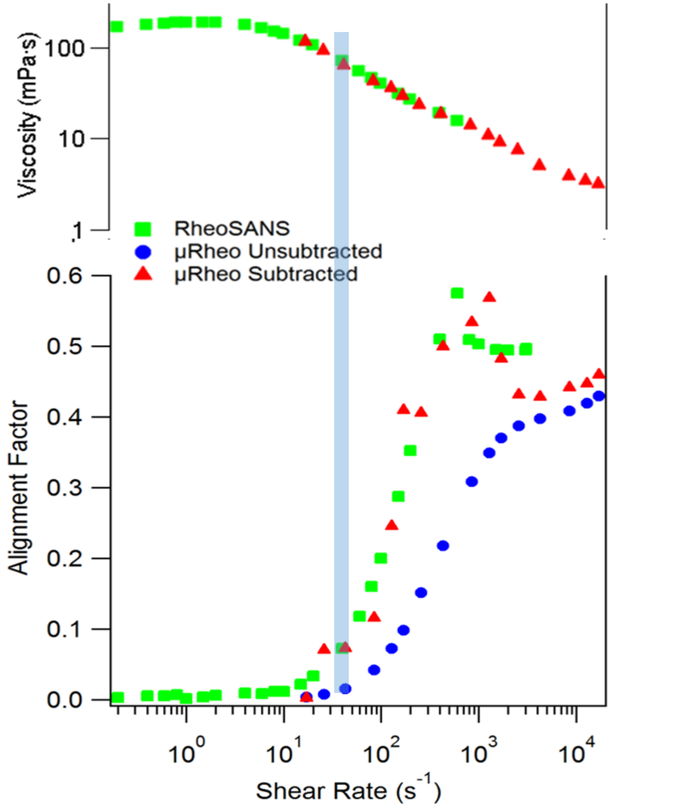

$$I_{q_x,q_y}(wall) = \frac{1}{1 - \frac{\tau_{\mathrm{wall,n-x}}}{\tau_{\mathrm{wall,n}}}}\left[I_{q_x,q_y}(Q_n) - \frac{\tau_{\mathrm{wall,n-x}}}{\tau_{\mathrm{wall,n}}} I_{q_x,q_y}(Q_{n-1})\right]$$

Fernandez-Ballester et al, *J. Rheology*, 2009, 53, 1229

Analysis: Determining Structure near the Wall

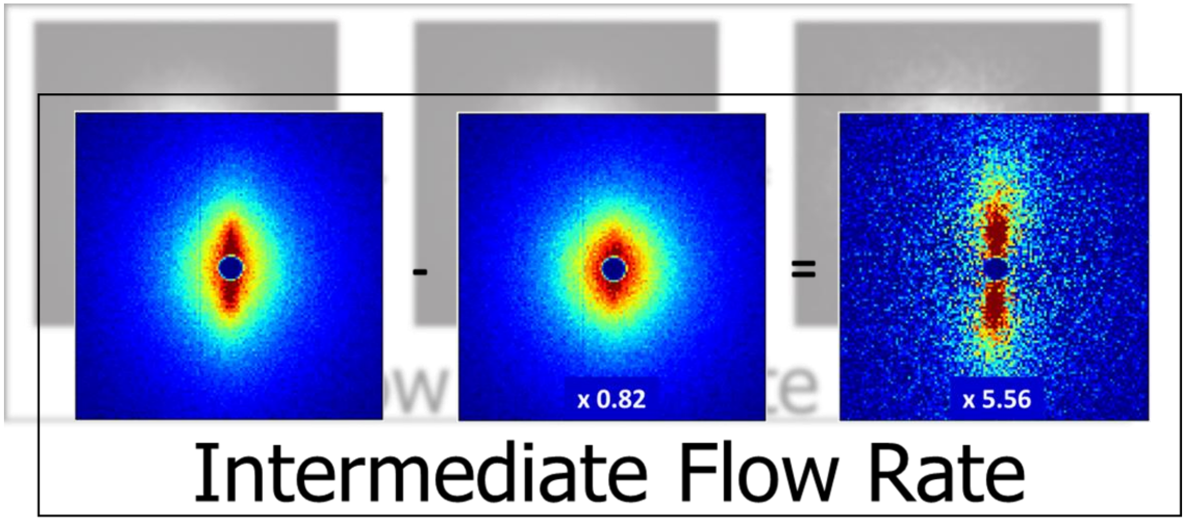

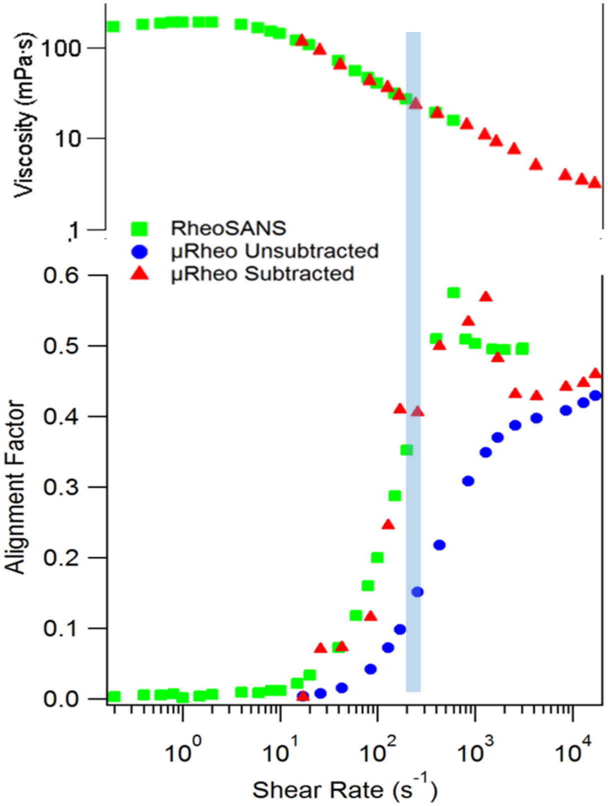

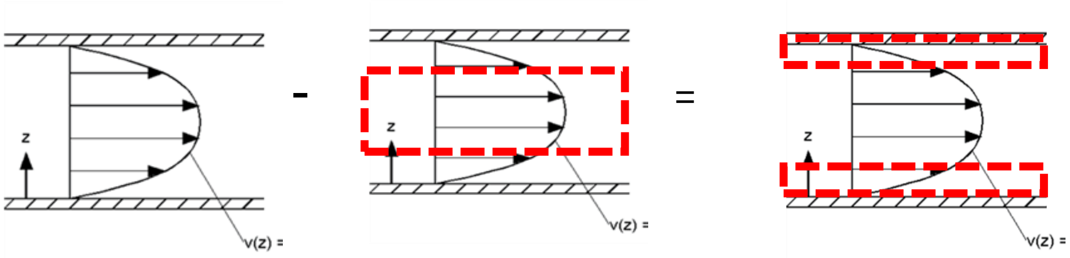

Fernandez-Ballester et al, *J. Rheology*, 2009, 53, 1229

Analysis: Determining Structure near the Wall

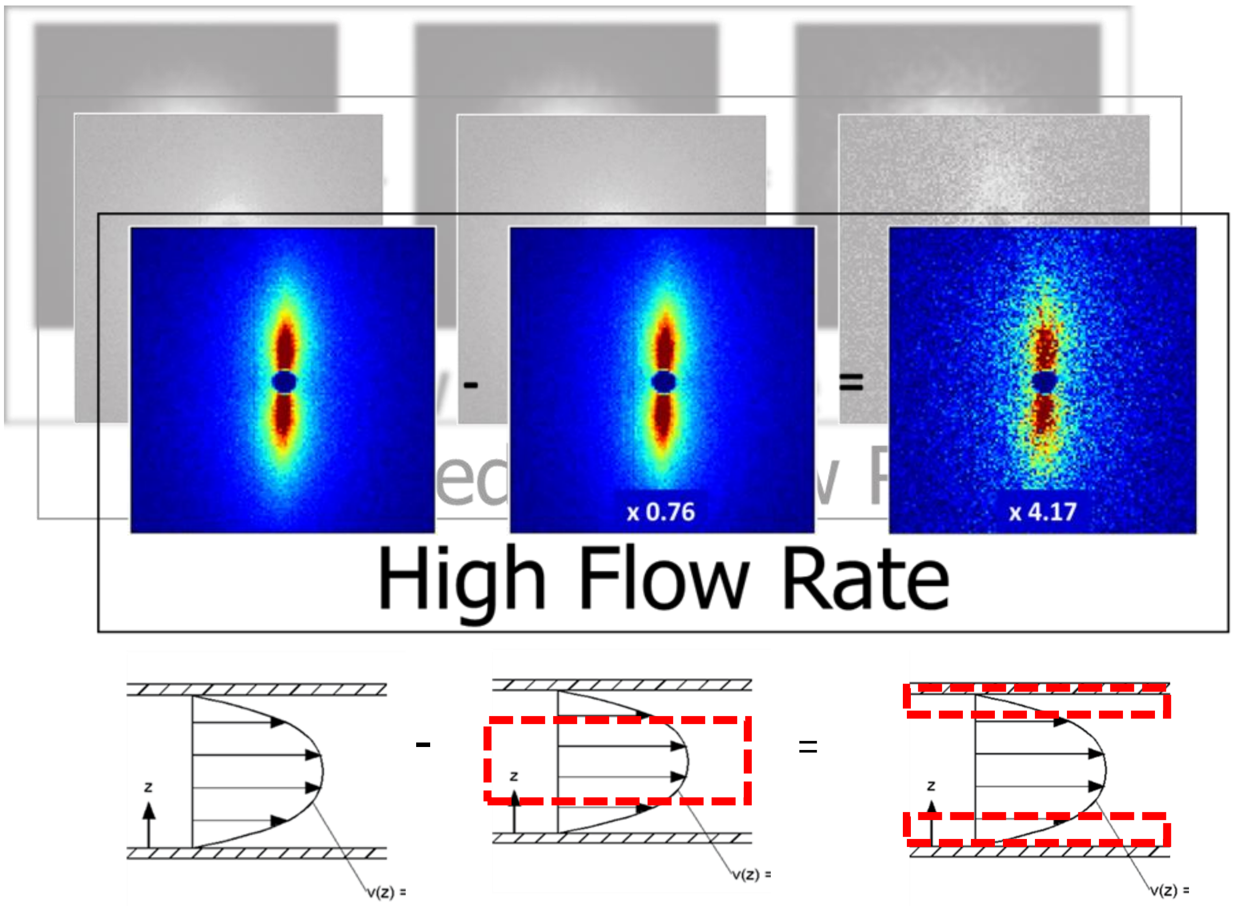

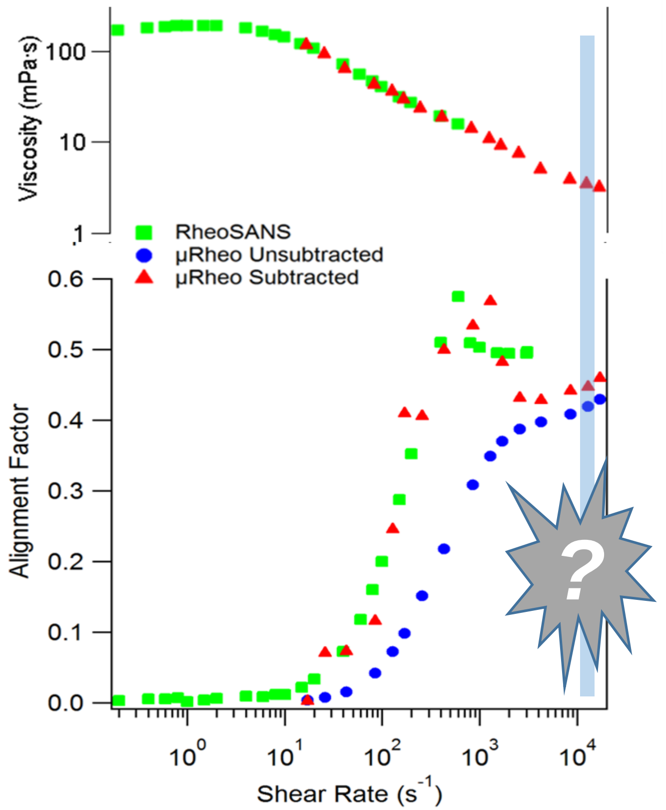

Fernandez-Ballester et al, *J. Rheology*, 2009, 53, 1229

μRheoSANS of Anionic Wormlike Micelles

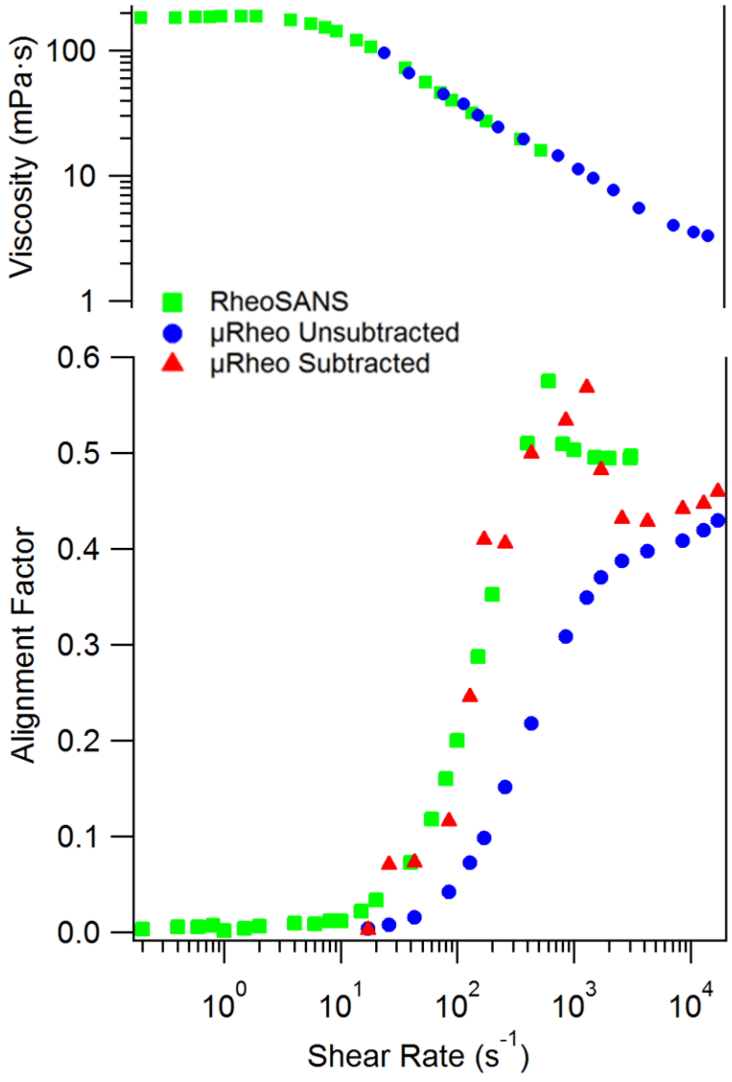

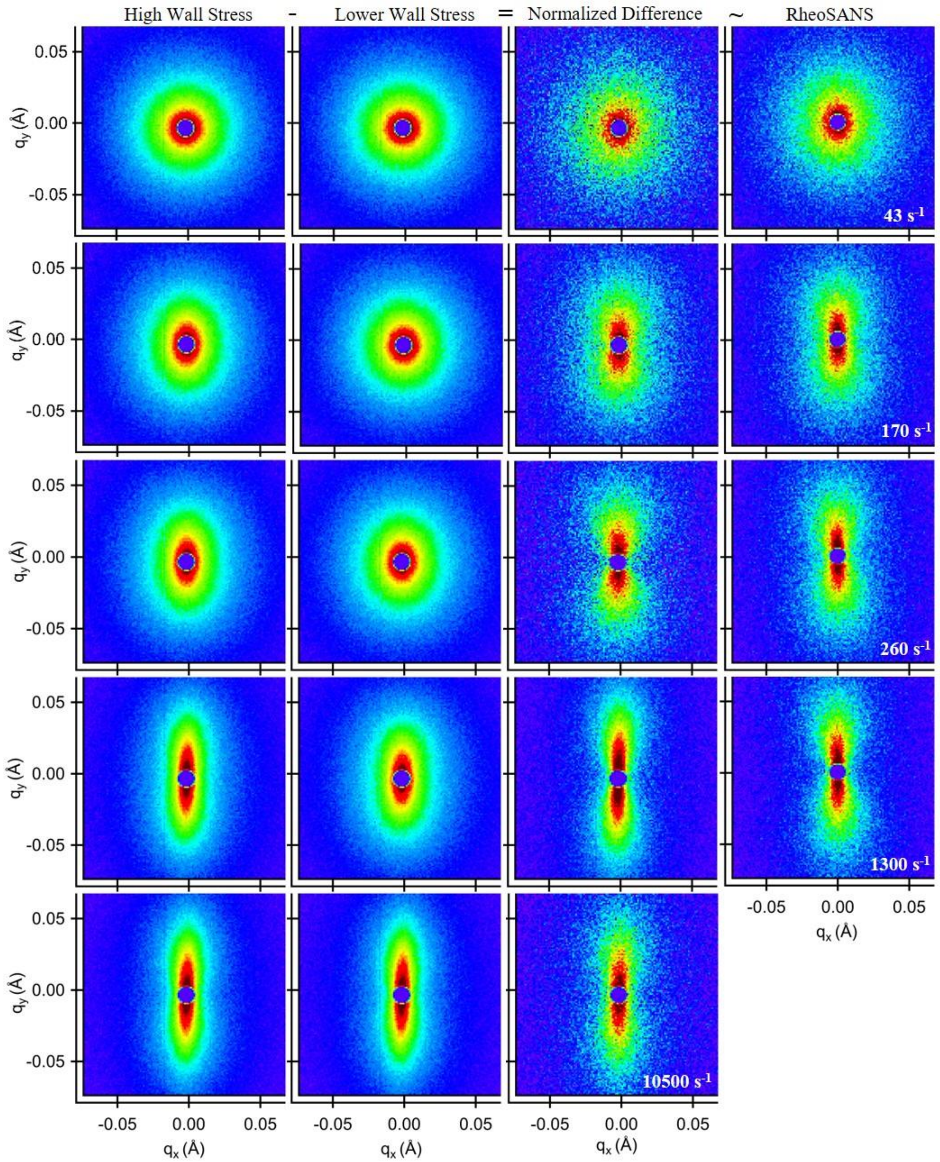

High shear SANS in rectangular channels

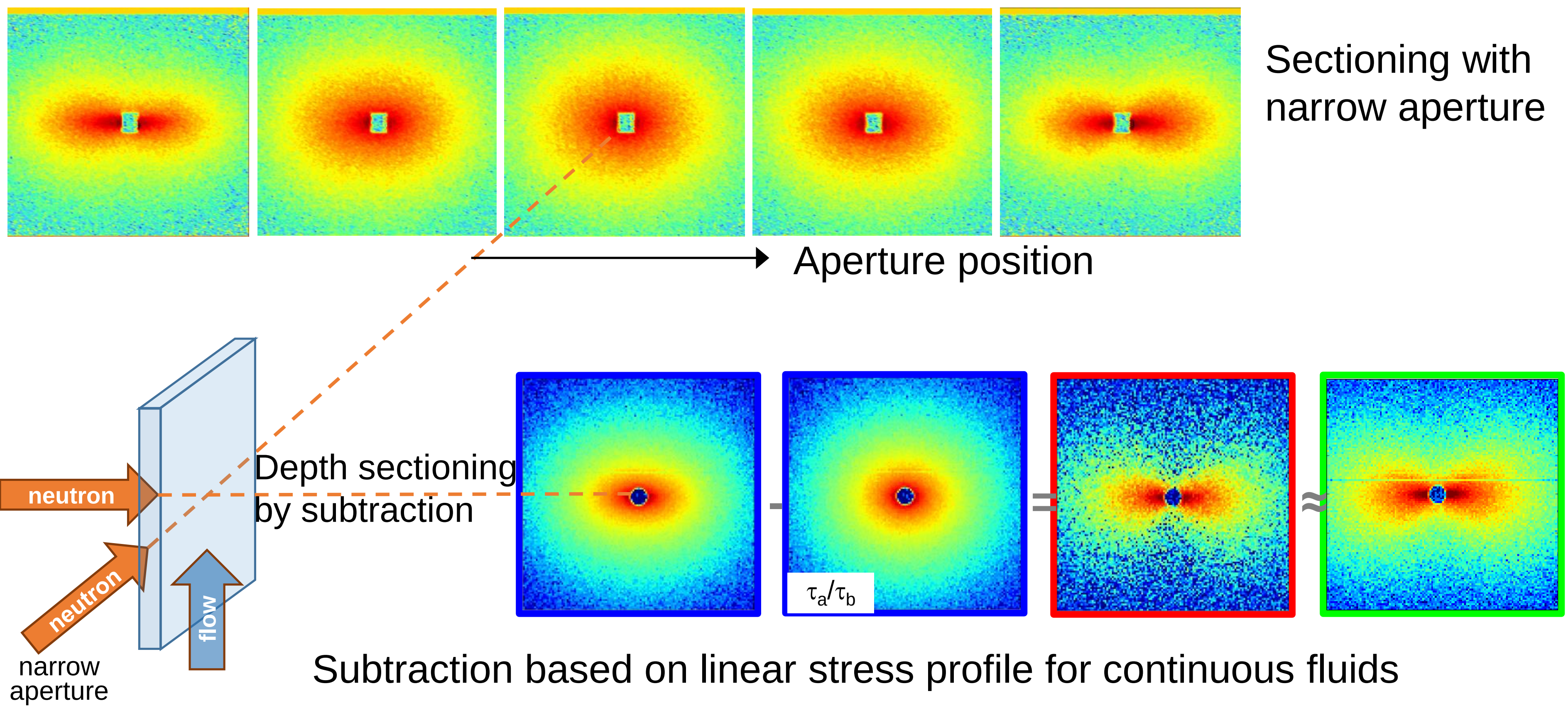

Slit scan data from D22 at ILL in collaboration with Lionel Porcar and Joao Cabral

μRheoSANS Limitations

- Depth dependent scattering analysis:
  - Approach will fail if the scattering depends on position independent of stress
    - Concentration gradient
    - Continuous sample (no sample fracture)
  - Slice depth relative to scattering object dimensions
  - Time…
- Pressure drop or flow rate limited in terms of reaching high shear rates…

μRheoSANS -- Prototype

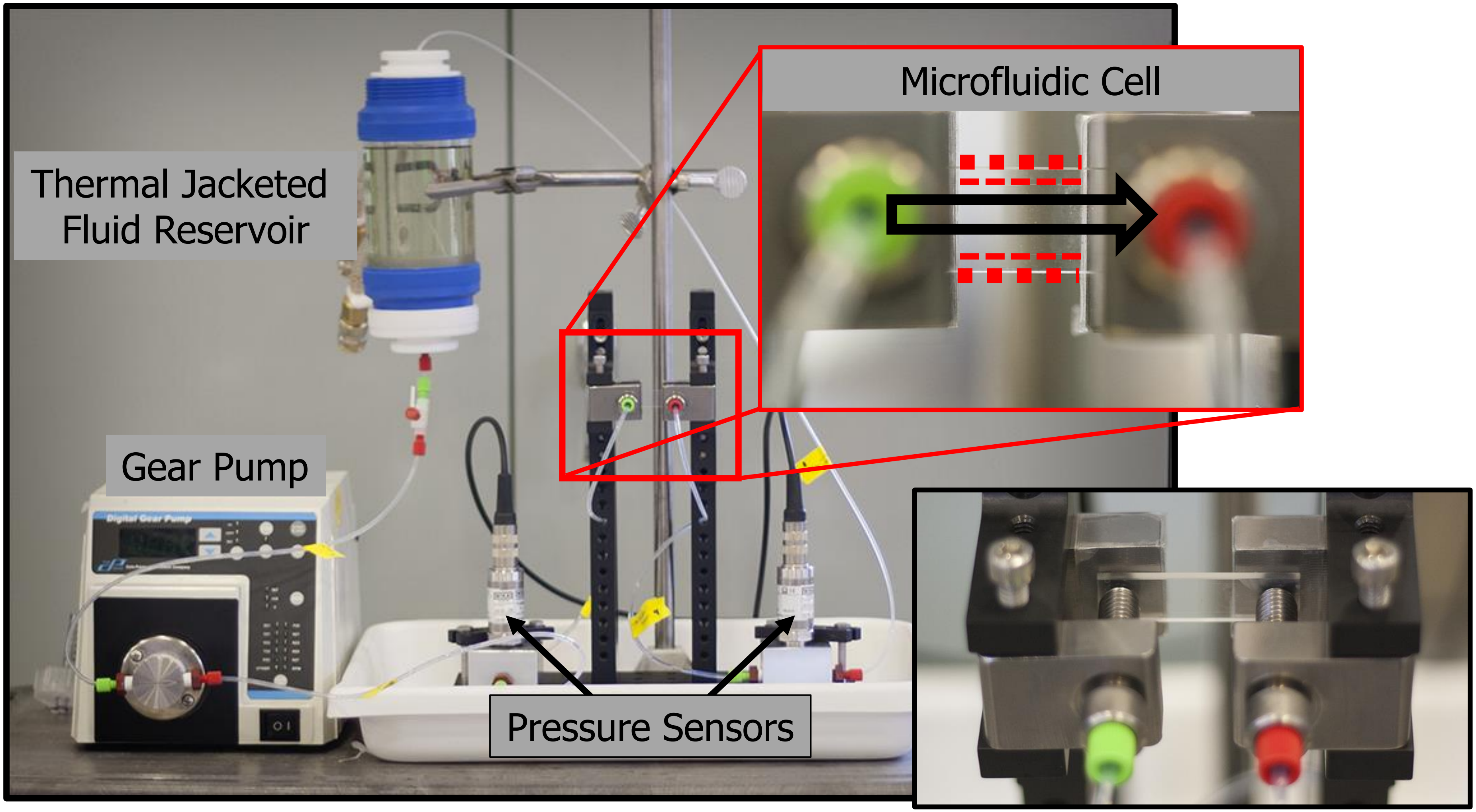

Weston, Seeman, Salipante, Blair, Hudson and Weigandt (In Preparation)

μRheoSANS Upgrade (high P/SR)

Fluid	Maximum Shear Rate, s^{-1}			Maximum ΔP, psi		
	25 μm	50 μm	100 μm	25 μm	50 μm	100 μm
Water	4.25×10^6	1.07×10^6	2.67×10^5	3500	450	60
Ethylene Glycol	3.08×10^6	1.07×10^6	2.67×10^5	5000	5000	1083
Glycerol	4.10×10^4	8.21×10^4	1.65×10^5	5000	5000	5000

*based on a rectangular channel 15 mm wide x 70 mm long

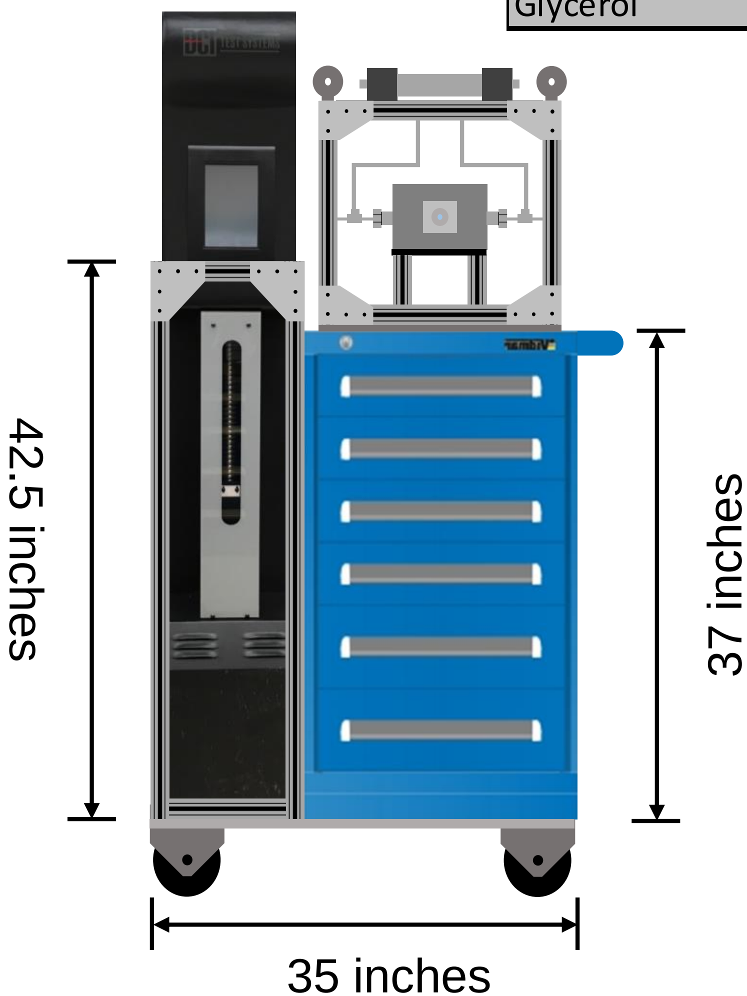

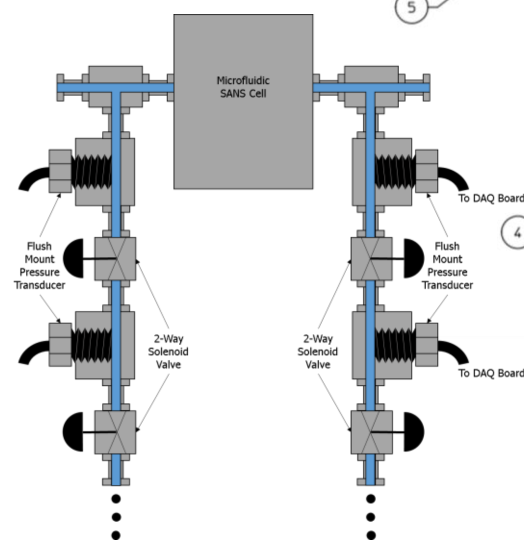

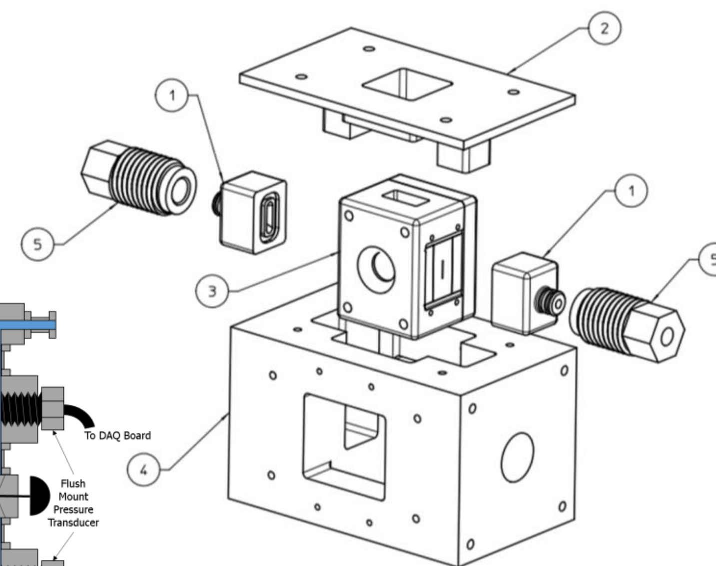

µRheoSANS Upgrade (high P/SR)

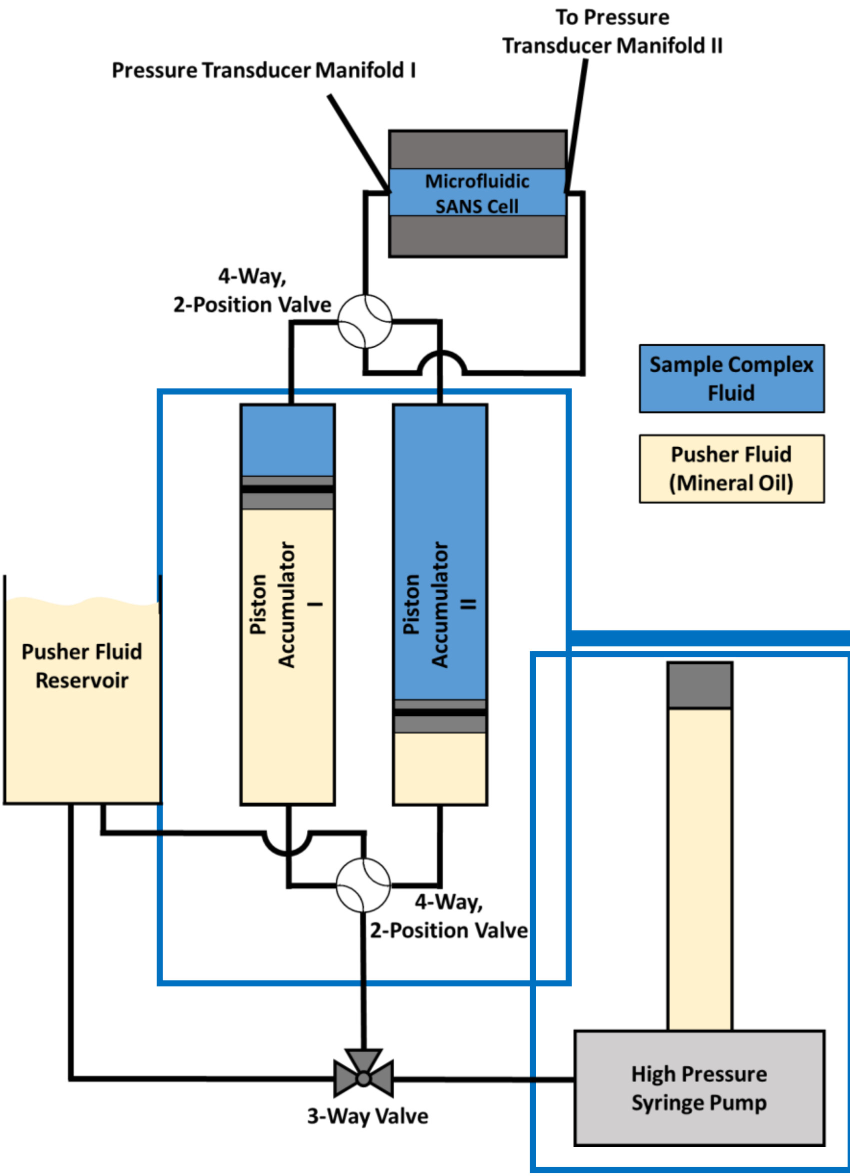

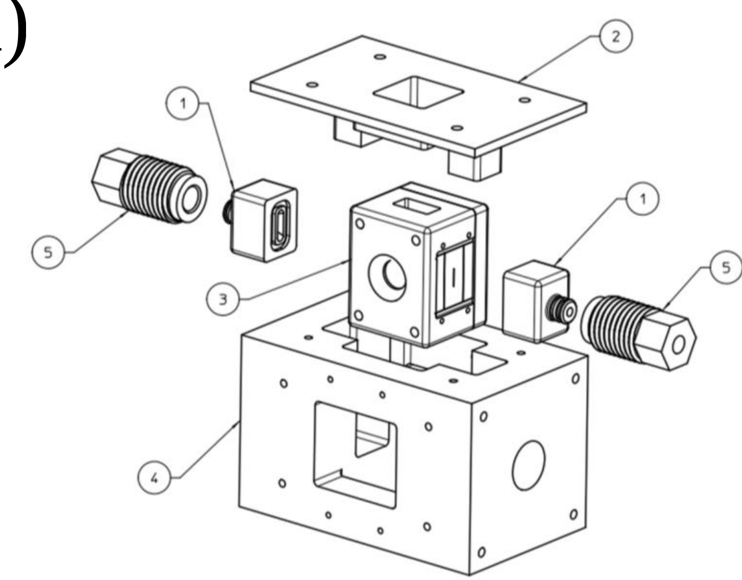

HiP Tubular Reactor w/Piston

- 125 mL each
- 10 000 psi – 700 bar
- 304 Stainless Steel
- 0 – 125°C

DCI VPA Syringe Pump

- 400 mL/min
- 5000 psi – 345 bar
- Stainless Steel Cylinder
- 12 nL volume resolution

Challenges

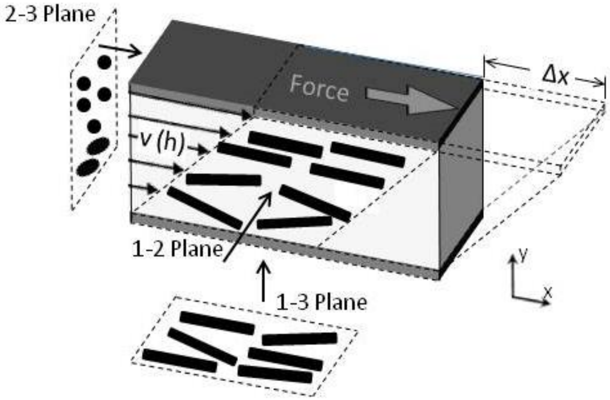

Analysis: Can we get more from our anisotropic 2D data?
Simultaneous fits of data through multiple flow planes?

Limitations: Communicating limitations without stifling creativity?

Portability: How easy is it to port new sample environment from one facility to the next?

Extra Slides

Microfluidics-SANS

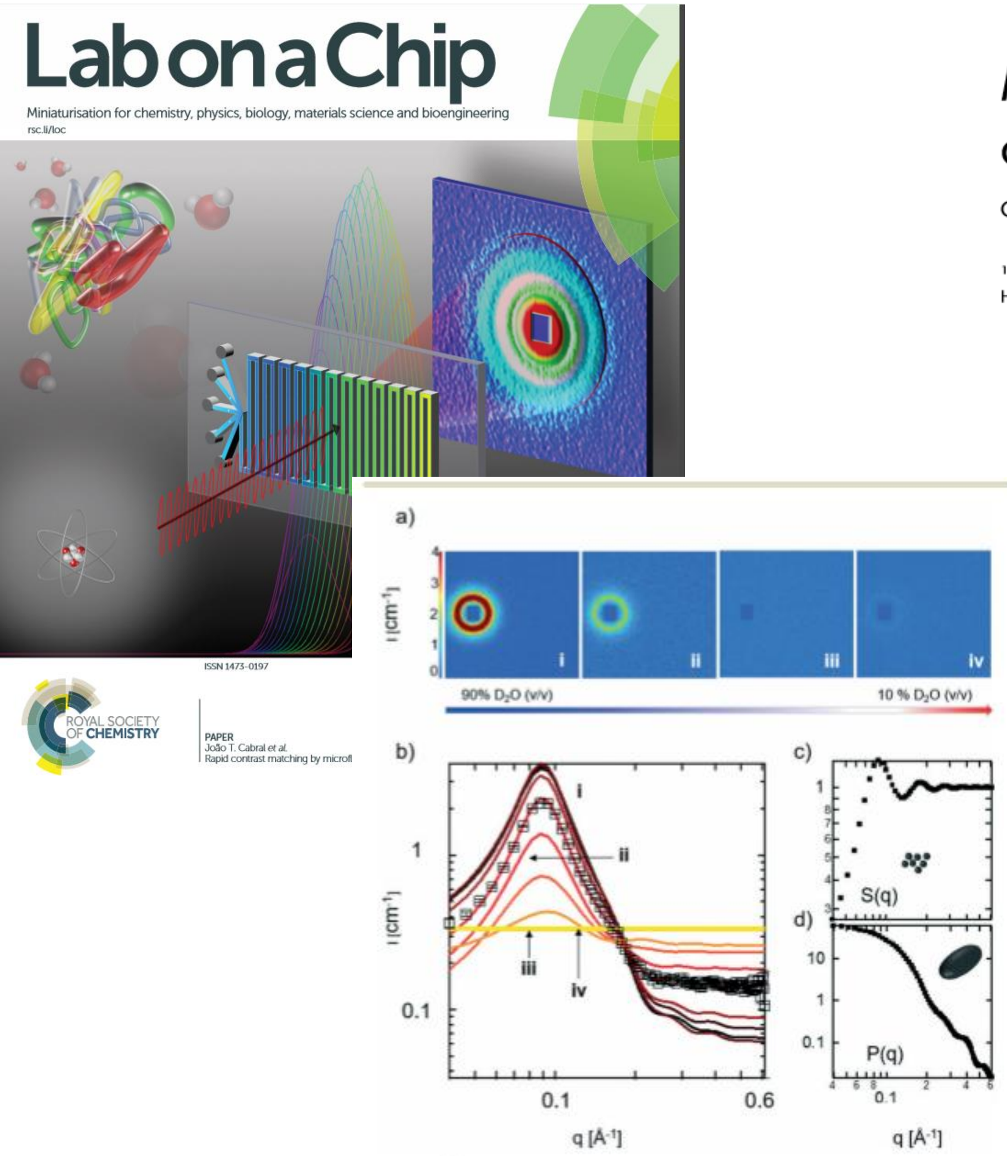

Microfluidic-SANS: flow processing of complex fluids

Carlos G. Lopez[1], Takaichi Watanabe[1], Anne Martel[2], Lionel Porcar[2] & João T. Cabral[1]

[1]Department of Chemical Engineering, Imperial College London, London SW7 2AZ, UK, [2]Institute Laue-Langevin, BP 1566 rue Jules Horowitz, 380 42 Cedex 9 Grenoble, France.

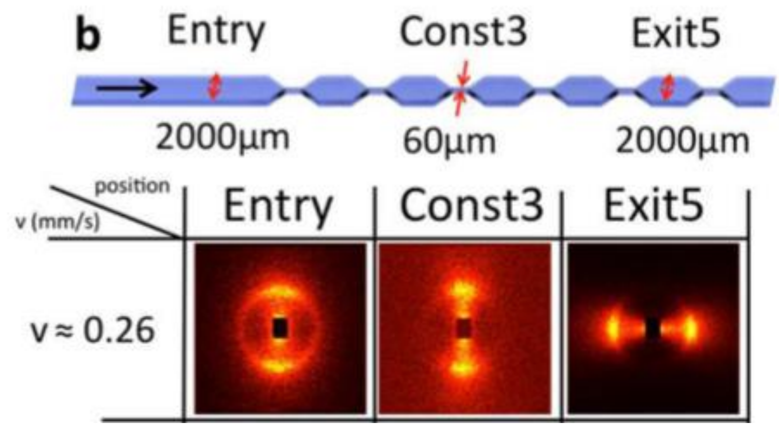

Joao Cabral and Lionel Porcar et al

Millifluidic SANS -- SANSdrop

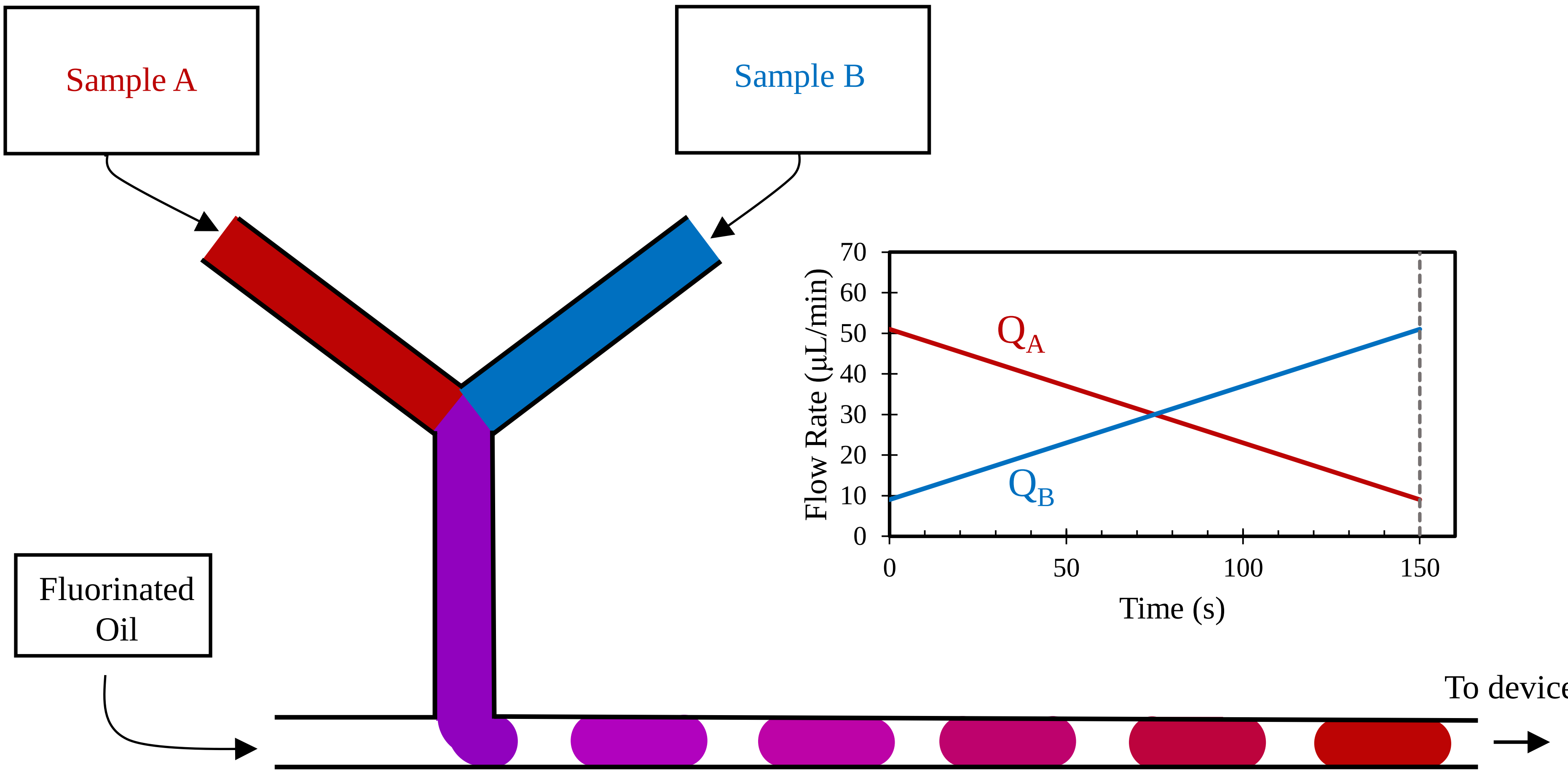

- Vary individual syringe pumps to produce concentration gradient
- Keep combined dispersed phase flow rate constant